Full Length Article

# Implications of lattice structures on economics and productivity of metal powder bed fusion

Iñigo Flores[a],*, Niklas Kretzschmar[b], Abdul Hadi Azman[c], Sergei Chekurov[b], David Bue Pedersen[d], Atanu Chaudhuri[e]

[a] *Section of sustainable production, Department of Engineering Design and Production, School of Engineering, Aalborg University, Copenhagen Campus (Denmark)*
[b] *Department of Mechanical Engineering, School of Engineering, Aalto University, Espoo (Finland)*
[c] *Centre for Integrated Design for Advanced Mechanical Systems, Faculty of Engineering and Built Environment, Universiti Kebangsaan Malaysia, Bangi, (Malaysia)*
[d] *Department of Mechanical Engineering, Technical University of Denmark, Lyngby (Denmark)*
[e] *Business School, Innovation and Technology Management, Durham University, Durham (England)*

## ABSTRACT

The cost-effectiveness of metal powder bed fusion (PBF) systems in high-throughput production are dominated by the high cost of metallic powder materials. Metal PBF technologies become more competitive in production scenarios when Design for Additive Manufacturing (DfAM) is integrated to embed functionality through shape complexity, weight, and material reduction through topology optimization and lattice structures.

This study investigates the value of DfAM in terms of unit cost and manufacturing time reduction. Input design parameters, such as lattice design-type, part size, volume fraction, material type and production volumes are included in a Design-of-Experiment to model their impact. The performance variables for cost and manufacturing time were assessed for two scenarios: (i) outsourcing scenario using an online quotation system, and (ii) in-house scenario utilizing a decision support system (DSS) for metal PBF.

The results indicate that the size of the part and the lattice volume fraction are the most significant parameters that contribute to time and cost savings. This study shows that full utilization of build platforms by volume-optimized parts, high production volumes, and reduction of volume fraction lead to substantial benefits for metal PBF industrialization. Integration of DfAM and lattice designs for lightweight part production can decrease the unit cost of production down to 70.6% and manufacturing time can be reduced significantly down to 71.7% depending on the manufacturing scenarios and design constraints when comparing to solid infill designs. The study also provides a case example of a bracket design whose cost is reduced by 53.7%, manufacturing time is reduced by 54.3 %, and the overall weight is reduced significantly with the use of lattices structures and topology optimization.

## 1. Introduction

Additive manufacturing (AM) is considered to be one of the pillars of the fourth industrial revolution [1]. Metal powder bed fusion (PBF) systems have become a niche competitor to conventional manufacturing processes, especially for manufacturing scenarios that require flexibility, small-lot production, mass-customization applications, and functionally enhanced components [2]. An increasing number of original equipment manufacturers, large companies, and small and medium enterprises are incorporating metal PBF systems in their industrial production workflows [3].

Concurrently, engineers and researchers are using the new design freedom of AM to produce enhanced components or entire assemblies which were previously impossible or impractical to manufacture [4]. To achieve an improved design for successful technology integration, engineers need to understand the principles of Design for AM (DfAM) [5]. The potential uptake of AM as an alternative manufacturing solution is dependent on the ability to integrate DfAM opportunities in the engineering design process.

Demonstrators of DfAM for industrial applications include the production of complex hydraulic manifolds with higher efficiency and decreased pressure drop [6] or optimized heat exchangers that allow maximizing efficiency by reducing the part volume [7]. DfAM opportunities also relate to part consolidation, which is the process of simplifying product assemblies by means of consolidating its parts into a minimal set of elements while maintaining its functionality [5].

---

* Corresponding author.
  *E-mail address:* ifi@m-tech.aau.dk (I. Flores).

The opportunities for AM are not only limited to enhanced and optimized products. The success of any given AM business case needs to be measured by combining both technological as well as operational aspects [8]. From the operational perspective of a company, AM provides opportunities to streamline product development processes [9], supply chain structures [10], and performance of the entire value chain [4]. Additionally, AM can be used to digitalize manufacturing processes to gain in productivity, especially when there is a need for mass-customization [11] while reducing inventories by enabling on-demand manufacturing schemes that reduce the need of stock-keeping units and physical inventories [12]. Ultimately, the combination of technical with economic feasibility studies are decisive in determining whether AM can compete with existing manufacturing solutions [11,13,14].

The competitiveness of metal PBF in manufacturing depends significantly on material cost savings [15,16]. Therefore, topology optimization and lattice structures are notable technical opportunities that have become enablers for AM technology adoption in end-use part manufacturing due to their ability to reduce the weight of parts [4]. Topology optimization and lattice structures are especially important in components that are redesigned for AM to reduce their weight [17] and in components that are designed directly for AM, where they can be used to engineer functionally enhanced products [18].

The existing literature on cost modelling for AM is focused on presenting the cost structures in production through exemplary parts and case studies. The costs of AM are commonly calculated with raw materials (including sacrificial support structures) as a direct cost, machine cost allocated through build time as an indirect cost, and labor as a separate fixed cost [19]. The degree of machine utilization and the ability to fully utilize the machine build volume for batch production is also included in existing AM cost models [16].

In typical case studies, the cost of producing components with AM is calculated and compared to the cost of conventional manufacturing using break-even point analysis [20]. For example, a customizable automotive plastic gripper part is used to demonstrate that AM is more cost-effective in producing components with many variations because injection molding requires costly tools for every product alternative [11]. In another case study, part consolidation was used to compare the cost-effectiveness of AM with injection molding. This investigation was based on an electric component that was redesigned to capitalize on the design freedom of AM [21]. Similarly, a slightly modified metal stainless steel hot air blower was shown to be more cost-effective to produce with AM than conventional manufacturing after applying part consolidation [19].

The machine utilization rate and build volume rate (BVR) are relevant metrics of productivity of metal PBF systems [22]. Best in class commercial PBF systems are capable of producing parts with build volume rates up to 27.78 mm$^3$/sec [23]. Material cost dominates the cost of production at build volume rates above 20 mm$^3$/sec [15]. In a case study presented by Kretzschmar et al. [15], the material costs accounted for 63% of the total cost per part at high BVRs. The remaining costs are related to machine and labor, which are responsible for 26% and 11% of the final unit cost, respectively [5]. The exact cost distributions are highly dependent on specific AM designs, machines, and materials. Nevertheless, the high relevance of material cost in high productivity scenarios applies to all metal PBF systems.

The cost of parts produced with metal PBF systems in industrial settings is therefore primarily determined by the high price of the machinery and metallic powder materials. Therefore, production cost can only be decreased by either reducing the need of material from the original design (e.g. part weight reduction through DfAM), or by enhancing the productivity rates of the machines (e. g. set-up times, full utilization of the build volume and increased build volume rates to obtain higher productivity).

The principal objective of this research is to study the impact of lattice structure design on the economics of metal PBF. This research provides an overview of cost reduction limits and saving potentials for

the AM of end-use components using metal PBF. The work is limited to study productivity issues of DfAM using lattice structures and topology optimization; and therefore, it does not perform an in-depth study of the technical feasibility and mechanical performance analysis of lattice designs. The implementation of lattice structures requires careful examination to ensure manufacturability and that the functional requirements of the product remain fulfilled in real engineering applications.

The value of DfAM (i.e. productivity and economics) in regard to lattice structures is determined through a Design-of-Experiments (DOE) approach that varies 5 different independent variables (i.e. lattice type, part size or bounding box, lattice volume fraction, production volume, and material), and measures two dependent variables (i.e. manufacturing cost and manufacturing time). The dependent variables are estimated for two manufacturing scenarios. The first scenario involves the outsourcing of metal PBF to service providers, whereas the second scenario consists of the use of in-house AM production that is linked to a developed online decision support system (DSS). Additionally, a bracket re-design case study is presented as a baseline case to evaluate and corroborate the findings of the DOE, while assessing potential benefits of DfAM integration with a real example.

### 1.1. Design opportunities for metal lattice structures

Lattice structures are primarily used to achieve high strength/low mass ratios by replacing solid material in parts [24]. Depending on their bending or stretching mechanical properties, lattices can also be used in the design of high-strength or energy-absorbing components [25]. Lattices are defined by an elementary structure, which is repeated in the three-dimensional design space. Many design configurations and design variables need to be considered when integrating lattices into part designs. This involves lattice structure pattern, volume fraction, section thickness, element length, gradience, and conformity [26].

As an example of common AM lattice structures, Fig. 1 shows three elementary lattice designs as well as a periodical octet-truss lattice design. Lattice or cellular structures were previously manufacturable through manufacturing techniques such as casting [27], snap-fitting [28], and metallic wire assembly [29]. However, these processes were complex, expensive, and had to respect several design restrictions,
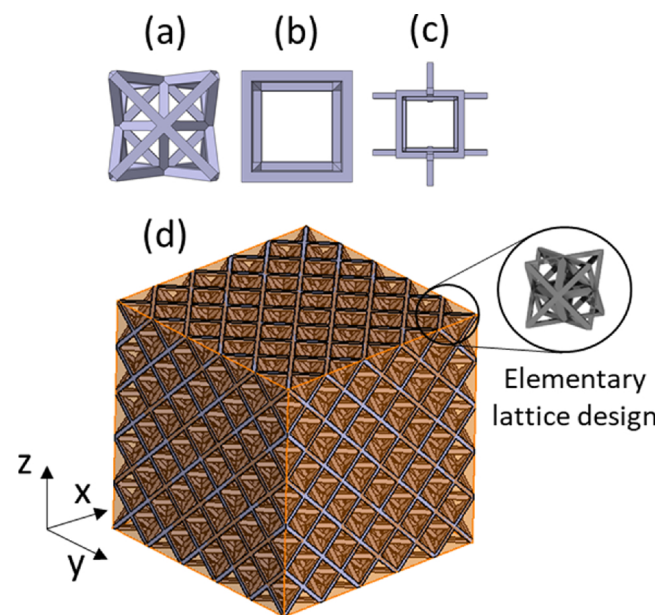


**Fig. 1.** Examples of lattice designs. (a) octet-truss design, (b) cubic-truss design, (c) open-cell lattice design, and (d) a periodical lattice structure with an octet-truss design and a volume fraction of 0.15.
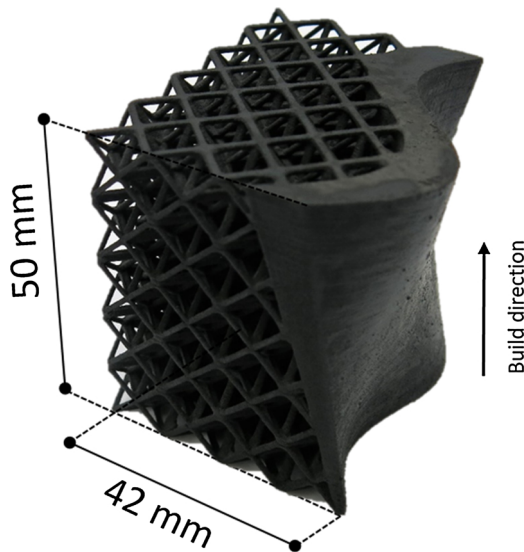
**Fig. 2.** Surface-lattice integration. A conceptual prototype for DfAM integration manufactured with selective laser sintering (SLS) of PA11 powder.

outweighing the lightweight benefits of lattice structures. Thus, they were not widely used despite their advantages [30]. Due to the progress in AM, more complex lattice structures can be efficiently manufactured today [31,32].

Fig. 1 (a) shows an octet-truss lattice element that is mechanically suitable to support loads in multiple directions. Fig. 1 (b) shows a cubic lattice design, which has stretching-dominated mechanical properties and it is best fitted for structures which are able to withstand a large load in a single direction. Fig. 1 (c) shows an open-cell lattice design, which is bending-dominated and suitable for energy absorption [33,34]. An essential parameter applicable to all lattice designs is the volume fraction (VF) ratio that is defined as the ratio between lattice structure volume divided by the bounding volume (Eq. 1).

$$Volume\ Fraction\ (VF) = \frac{Lattice\ structure\ volume}{Bounding\ box\ volume} \quad (1)$$

A volume fraction (VF) equal to 1 represents a solid structure. The purpose of decreasing volume fractions is linked to the goal to minimize the amount of material being used for the print and to reduce its overall weight. Fig. 2 shows a conceptual example of a lattice design applicable to end-use parts to decrease weight while maintaining geometrical and mechanical functions of the part. The inner core of the part is designed with octet-truss based lattice structures (VF = 0.15) while the outer surface remains solid, thus reducing its overall weight and keeping its functionality.

### 1.2. Manufacturability of metal lattice structures

During the engineering design phase, an understanding of the inherent limitations of the metal PBF process is required to ensure reliable manufacturing of lattice structures. One of the critical aspects of designing parts for metal PBF is that the un-melted powder must be removed after manufacturing. Previous research shows that common lattice structures such as cubic and octet-truss are limited to volume fractions that cannot exceed 0.3 to ensure the removal of un-melted powder through escape holes [25]. Another limitation relates to the highest achievable resolution of metal PBF. Volume fractions below 0.15 require that the geometrical features of the lattices be close to the highest achievable feature resolution. Nevertheless, these assumptions can be challenged as the design rules for lattice designs are material, process, and geometrical design-dependent [35].

A rather conservative set of design rules for metal PBF recommend a minimum wall thickness of 0.4 mm to ensure a successful build. Finer structures are possible, but dependent on orientation, material, and process parameters [36]. In the case of geometrical features, such as unsupported edges or strut lengths, the maximum length of a cantilever-style overhanging surface is 0.5 mm and an overhanging horizontal surface supported from both ends can have a length of 1 mm. Many other design rules based on empirical observations of the success of builds relevant for lattices are reported for escape holes [37,38] and powder removal [38].

The definition of design rules for lattice structures is interlinked with the material, process parameters and part orientations [39]. An optimal DfAM strategy would consider them all to define a build strategy that minimizes the residual stresses and the risk of build failure by maximizing heat dissipation. Thus, reducing unnecessary heat exposure during the manufacturing process, avoiding heat-induced geometrical distortions that can lead to crashes between the recoating system and the part during the build process as well as dimensional deviations of produced components [39]. Another critical parameter that limits AM applications is the build volume size of commercial AM systems, which is 250 mm x 250 mm x 300 mm on average [37].

Fig. 3 shows two examples of lattice structures that are challenging in terms of manufacturability. They were manufactured from stainless steel 1.4404 using a ConceptLaser MLab Cusing R metal PBF machine with a building envelope 90 mm x 90 mm x 80 mm and a 100 W fiber laser. The layer thickness of the process was set to 25 μm for high feature resolution. A laminated scanning pattern of 45° was required to fabricate the octet-truss lattice design of Fig. 3 (b) while an island scanning pattern with standard parameters was used to fabricate the cube-truss lattice design of Fig. 3 (a). Both lattice structures have a size of 50 mm x 50 mm x 50 mm with elementary lattice cell sizes of 10 mm x 10 mm x 10 mm. The volume fraction is 0.15 for both lattice types; minimum feature sizes amount to 0.611 mm in width for the cubic-truss design and 0.62 mm in the octet-truss design. Both lattice designs are at the edge of the earlier mentioned general design rules and manufacturability limits.

To ensure success in the manufacturing of the lattice design present in Fig. 3, the orientation during the build process is selected in such a manner that support structures inside the part are not present or minimized, since the removal of these structures in post-processing stages is difficult and time-consuming. In many cases, the removal of internal supports is impossible because of inaccessibility. To avoid internal supports, the cubic-truss lattice structure was reoriented by 45° rotations around the x and y-axis, the octet-truss lattice structure was printed as shown in Fig. 3 (b) (this structure always violates the 45° degree rule regardless of its orientation). Fig. 3 (c) shows small manufacturing defects in both lattice designs. The additively manufactured parts show visible defects, such as zones of unmelted powder and broken overhanging struts as well as a degree of inaccuracy and geometrical distortion. However, overall, both cases demonstrate that it is possible to manufacture lattice designs with a low volume fraction of 0.15, reduced geometrical feature size and 90° overhangs (i.e. horizontal struts of the octet-truss based structure).

Overall, a combined engineering workflow of design and manufacturing is required to successfully build parts with inner lattice structures and replaced solid structures [40]. Mathematically, there is no unique arrangement to design lattice structures as lattices can be composed of different unit cells and geometrical features. However, not all the lattice designs are feasible for manufacturing in metal PBF. Design rules, unit cell orientation in relation to the build orientation, process parameter optimization, and the applied strategy for secondary finishing operations (e.g. heat treatment for stress relief) define the feasibility in their production. Fig. 3 shows two exemplary cases of lattice designs. These designs and manufacturing experiments are not representative for the overall design space. As a consequence, to
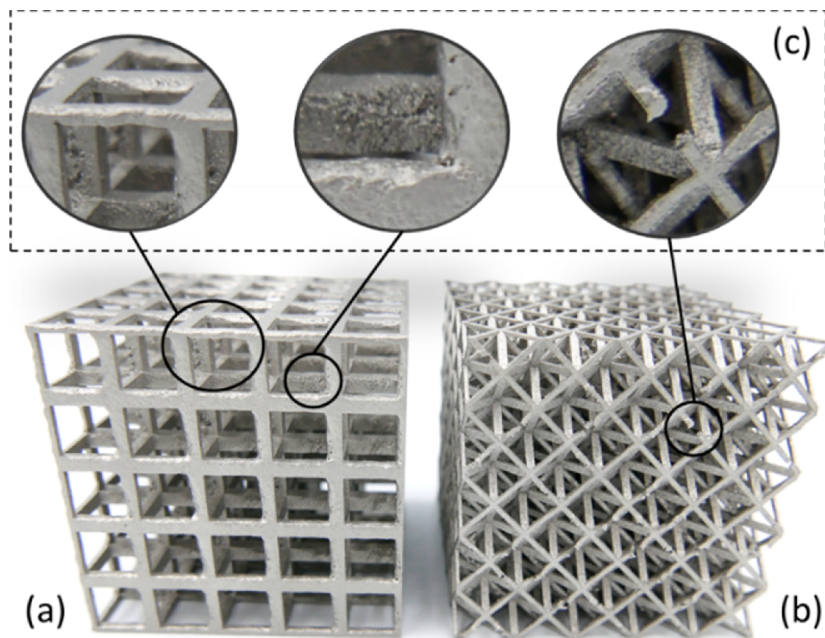
**Fig. 3.** Lattice structure examples manufactured by metal PBF. (a) cubic-truss lattice structure with a volume fraction of 0.15 and a bounding box of 1000 cm³. (b) octet-truss lattice structures with a volume fraction of 0.15 and a bounding box of 1000 cm³. (c) Manufacturing defects including warping, unsintered powders and flat edges, and broken struts (from left).

succeed in the manufacturing of lattice structures with a different type of unit cell and geometrical features other than the ones presented in this research, a detailed study on manufacturability is required.

### 1.3. Manufacturing time and productivity of metal lattice structures

Production volume has an effect on productivity as the build platform of metal PBF machines has a reduced size; thus high production volumes require to be processed in batches enabling full utilization rates of the build platform [16,41]. Build volume rate (BVR) is a measure of how much material volume is created from the metal powder over time. It is a productivity parameter used to compare different AM systems [15]. BVR in metal PBF is the result of complex interrelationships between physical, process, and material interactions. Beam power, energy absorption rate, scanning speed, scanning patterns, layer thickness, and recoating speed, are among the most relevant variables that define BVR and feature resolution [42]. As a rule of thumb, increased layer thicknesses require higher energy density levels and higher laser penetration depths, and therefore, resulting in reduced accuracy with the benefit of increased BVR.

Small geometrical details are required to produce lattice structures using metal PBF. In practice, the smaller the layer thickness, beam diameter, and the power of the laser, the smaller the geometrical details that can be produced [43]. It is possible to reduce the overall part volume and therefore the area per slice that requires to be processed by using lattices to replace solid material in metal PBF. As an example of this, Fig. 4 (a) shows a comparison between an octet-truss lattice design (VF = 0.15) with a fully filled part (VF = 1). Fig. 4 (b) shows a representation of the midplane cross-section area and the scan area for both lattice designs, octet-truss and cube. Fig. 4 (c) illustrates the layer thicknesses and an example of a scanning pattern. Comparing the two cross-section areas presented in Fig. 4 (b), the scan area per slice is reduced from 100 cm² to 6.2 cm², thus decreasing the scanning time per layer and the overall manufacturing time.

## 2. Research design

### 2.1. Design of experiment

In order to evaluate the impact of lattice variables, the cost and manufacturing time are modeled with a data-driven modelling approach using Design of Experiments (DOE). Table 1 outlines the selected independent variables of the study. A cube primitive with equal lengths on all three axes was modified according to the 108 experimental combinations described in the full factorial DOE. The cube is used as an abstraction of a product designed for AM. The measured responses or dependent variables are the unit cost of production and the manufacturing time. We refer to the dataset in the Table A1 in Appendix A to evaluate the findings, replicate, and verify the results independently.

The included independent variables are: (i) the lattice type (LT) as a categorical variable that describes two common lattice types, uniform cubic-truss (C) and uniform octet-truss (O), (ii) the size of the bounding box of the cube (S), 125 cm3 and 1000 cm3, treated as a continuous variable, (iii) the volume fraction (VF), 0.15, 0.3 and 1, treated as a continuous variable, (iv) the production volume (PV), 1, 10, and 100 units, treated as a continuous variable, and finally, (v) materials which were treated as a categorical variable corresponding to aluminum alloy "AlSi10Mg" (Al), tool steel "SS 1.4404″ (St), and titanium alloy "Ti6Al4V" (Ti). A single build orientation of the lattice designs is considered to avoid the need for internal support structures.

Fig. 5 shows the elementary unit cells of the lattice structures used in the DOE. The dimensions of both elementary unit cells (i.e. cubic-truss and octet-truss lattice designs) in x, y, and z have a length ($l$) of 10 mm in each dimension (i.e. $l_x = l_y = l_z$), which is kept constant for better comparison. The volume fraction (VF) of the obtained lattices bounding box is modified by changing the dimensions of the cross-section area of the struts proportionally; and therefore, maintaining the aspect ratio between strut width ($w$) and strut height ($h$).

Fig. 5 (a) shows the elementary octet-truss lattice design with a VF of 0.15 that has a strut width of $w_{Octet\,(0.15)}$= 0.62 mm, strut height of $h_{Octet\,(0.15)}$= 0.88 mm, and an unsupported beam length of 6.19 mm. Fig. 5 (b) shows the octet-truss lattice element with a VF of 0.3 that has a strut width of $w_{Octet\,(0.3)}$= 0.93 mm, strut height of $h_{Octet\,(0.3)}$= 1.32 mm, and an unsupported beam length of 5.76 mm. Fig. 5 (c) shows the elementary cubic-truss lattice design with a VF of 0.15 that has a strut width of $w_{Cubic\,(0,15)}$= 0.61 mm, strut height of 0.61 mm, and an unsupported beam length of 3.78 mm. Ultimately, Fig. 5 (d) shows the elementary cubic-truss lattice design with a VF of 0.3 that has a strut width of $w_{Cubic\,(0.3)}$= 0.91 mm, strut height of $h_{Cubic\,(0.3)}$= 0.91 mm, and an unsupported beam length of 3.18 mm. The manufacturability of the presented lattice structures is demonstrated in Fig. 3.
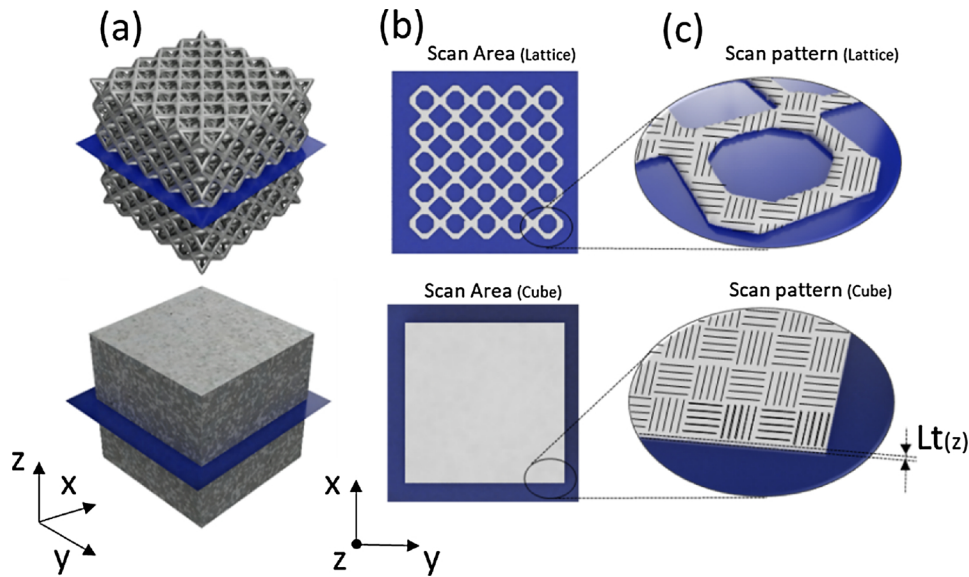
**Fig. 4.** Illustration of the impact of lattice structure design in productivity parameters. (a) Perspective view of an octet-truss lattice (VF = 0.15) and fully filled cube (VF = 1), (b) cross-section area of the lattice and the cube, (c) visualization of the layer thickness and scan pattern.

## 2.2. Modelling part-manufacturing cost

The economic impact of lattice structure design was modelled as follows: First, the cost of the outsourcing scenario (OUT) was modelled by uploading parts to an online quotation system for AM manufacturing services. In this case, the STL files of the designs were uploaded to an online tool that allowed to obtain the cost of a hypothetical outsourcing manufacturing scenario. The quotations were collected from Materialise (https://onsite.materialise.com/en) [44] for the analysis. In this regard, the methods for calculating the cost for the OUT scenario using the online quotation system are not known and confidential and are based on a company-specific pricing strategy. Furthermore, the resulting breakdown of manufacturing costs cannot be divided into cost structures as it only represents the purchasing price of parts manufactured by a service provider.

The second scenario, the evaluation of in-house (IN) manufacturing using laser PBF, was conducted using a decision support system (DSS) for metal PBF [15]. The DSS tool allows evaluating productivity factors (i.e., manufacturing cost and manufacturing time) for any given geometry. An online version of the DSS is accessible using this link (https://amdsp.org.aalto.fi). The DSS tool accounts for all three cost structures in metal PBF that include *machine cost*, *material cost*, and *labor cost*.

Firstly, in relation to *machine cost*: the underlying algorithm takes several parameters into account, such as (i) cost on machine purchase for 9 different metal PBF industrial systems, (ii) cost related to build preparation time, build job time, and build removal, and post-processing time including support removal. (iii) Overall recoating time, which is dependent on the layer thickness and part height, (iv) machine utilization rate, which represents that the PBF system is running 70% (i.e. 6120 h/year) of the time in a series production scenario, (v) maintenance cost for machine and software. Ultimately, (vi) we assume a
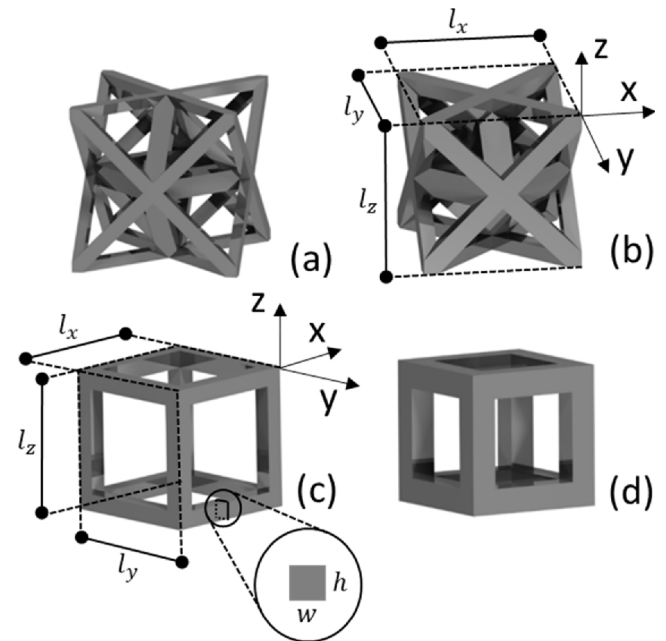


**Fig. 5.** Elementary unit cells of lattice structures, (a) octet-truss with a volume fraction of 0.15, (b) octet-truss with a volume fraction of 0.3, (c) cubic-truss with a volume fraction of 0.15, and (d) cubic-truss with a volume fraction of 0.30.

purchase depreciation of 8 years for the PBF machine and 5 years for related specialized software.

Secondly, in relation to *material cost*: the DSS calculations take into

**Table 1**
Lattice structure design and production variables.

| Variables | Nomenclature | Levels | | |
|---|---|---|---|---|
| Lattice type | LT | Cubic-truss (C) | | Octet-truss (O) |
| Bounding box (cm$^3$) | S | 5(x) x 5(y) x 5(z) = 125 cm$^3$ | | 10(x) x 10(y) x 10(z) = 1000 cm$^3$ |
| Volume fraction | VF | 0.15 | 0.3 | 1 |
| Production volume (units) | PV | 1 | 10 | 100 |
| Material | M | AlSi10Mg (Al) | SS 1.4404 (St) | Ti6Al4V (Ti) |

account, (i) cost of powder material purchase for three material alternatives, (ii) the cost of support structures are taken into consideration, (iii) the influence of batch production, calculating each time the number of parts fitting onto the build plate. The batch size; and therefore, the packing of parts is calculated by computing the X and Y dimensions of each part after automatic part orientation aiming at minimizing support structures versus the X and Y dimension of the build plate of selected machine. The resulting manufacturing cost is revealed by discrete and significant increases in the cost and build time as a function of production volume as the manufacturing moves from one batch to another. Finally, (iv) the powder recycling effect and resulting cost of waste material are considered due to its relevance in the resulting unitary cost of production [45]. This is obtained by calculating the difference between the volume of filled powder bed versus the utilized build volume that is dependent on the maximum height of the build. The DSS calculations assume that the material between batches can be recycled with an efficiency rate between 95% and 98% [46].

Finally, in relation to *labor cost*: the cost of labor is calculated as the product of the workers' paid time and the production labor cost per hour based on a Western European salary. In detail, the employee is paid for the setup time, the build preparation time of each batch, a monitoring time of 10% during the manufacturing process, and de-powdering as well as support removal steps. It is relevant to mention that the cost-modelling is limited to direct part production. Therefore, the DSS does not consider the cost of additional post-processing steps, such as heat treatments for stress relief and machining operations for increased dimensional accuracy. N. Kretzschmar et al. [15], provides more information and a detailed explanation of the assumptions, mathematical formulas, the calculations, the underlying algorithm, and the methodology behind the DSS. Fig. 6 outlines the user interface of the web-based DSS platform.

In the primary menu, (a) by clicking on the image, the user can upload a binary STL file of the design to analyze it from a technical (e.g. dimensional verification of the uploaded part) and economic viewpoint (e.g. cost structures and lead times). (b) There is the option to select among 9 different metal PBF machines, 3 material types, and 3 accuracy levels which influence achievable maximum build volumes, BVRs and consequently economics and productivity of metal PBF. The required support structure can also be included for accurate calculations, which is automatically computed based on the orientation and resulting overhanging features. (c) Alternatively, the manual setting menu allows to customize machine and material settings including variables such as machine price, build chamber volume, and material price. The DSS system can implement (d) logistics/storage and (e) conventional manufacturing considerations to compare economically additively and conventionally manufactured parts.

The calculation results are displayed after the user selects the options in the primary menu and clicks on the "show results" button. To this end, (f) displays the unit cost of production (blue line) as well as the comparison with conventional manufacturing (yellow line) in a break-even point analysis, (g) shows the manufacturing time as a function of the production volume as well as the results of the achievable batch size (i.e., number of parts: 14 in this case), (h) creates a stacked bar chart of cost structures (e.g. machine, material, labour, storage, logistics, etc.) which compares multiple AM technologies with conventional manufacturing, (i) shows the build time per part using alternative AM technologies, (j) presents future cost projections to estimate the feasibility of AM, and (k) presents a front and side view of the uploaded STL-file. In this case, the image is that of an octet-truss lattice design of 1000 cm³, the same model being printed and demonstrated in Fig. 3 (b).

For the purpose of this research, we have simulated the in-house manufacturing scenario by selecting the metal PBF system EOS M400 with a build volume of 400 mm x 400 mm x 400 mm and a total beam power of 1000 W for high production throughput. The high-accuracy mode was selected to simulate the manufacture of detailed features,

which is needed for lattice structures. This selection is consequently lowering BVRs but estimating more accurately the required process parameters to produce necessary small geometrical features. Since manufactured parts cannot contain inner supports, simulations with the DSS were conducted by omitting internal support structures in general, since Fig. 3 demonstrates that manufacturing without these structures is technically possible. Another relevant parameter in the simulation is the utilization rate of the machine, which is set to 70%. This means that the machine in the in-house manufacturing scenario has a very high utilization rate, thus having a positive impact on achievable production rates.

### 2.3. Modelling part-manufacturing time

The modelling of build volume rate (BVR) in laser-based metal PBF involves a wide array of process parameters. Those values are obtained for each material and processing condition by combining experimental methods and physics-based models [47]. The need to vary process parameters is due to the complex material-process-property relationships during the PBF process.

The ability to obtain fully dense parts is highly subordinated to variables, such as the required layer thickness, the degree of volumetric energy absorption, the reflectivity of the powder material, the particle size distribution, and melting behavior of the material [48]. A high-fidelity physics and melt pool geometry-based simulation can be used to model achievable BVRs [49–51]. Ideally, a BVR model that accounts for layer thicknesses of commercial metal PBF machines and volumetric energy density absorption of different materials could be used. However, physics-based models tend to be computationally expensive [52] and complex to implement into web-based DSS systems that require quicker and leaner calculations.

To solve this issue, Fig. 7 shows a simplification of BVRs as a function of the laser power of the AM system for three different materials. The model fits a linear regression model for BVRs for each material based on experimental data, which was obtained by consulting scientific literature [15]. All the data points needed to construct the BVR model were material and process optimization experimental results for Al, St, and Ti with different accuracy levels that led to fully dense parts (i.e., part density ≥ 99.5%) [15]. Fig. 7 also displays the density ellipsoid assuming the bivariate normal distribution. The density ellipsoid works as a graphical indicator of the correlation between BVR and laser power to predict where a given percentage of new observations is expected to lie.

The general assumption of this method and the underlying calculation of the DSS in terms of manufacturing time is that lower laser powers allow higher feature resolution due to the decreased layer thickness. Higher laser powers have increased layer thicknesses and therefore, higher BVRs at the expense of accuracy. While this assumption is not entirely accurate in many cases, the generalization allows to simplify the BVR calculations and obtain an estimation of the overall manufacturing time in a computationally economical manner.

Based on the collected data points and the underlying assumption, the linear fit shows that titanium alloys reach the highest BVRs, followed closely by aluminum alloys, and ultimately steel alloys. Typically, the manufacturing layer thickness for aluminum alloys and titanium alloys in most PBF machines is usually two times that of steel alloys, which means that steel alloys require two times as much laser processing time and two times the amount of recoating time compared to the same part made with aluminum or titanium alloys. In practice, the obtained BVR value is calculated when the user selects the accuracy level in the DSS in Fig. 6 (b). The back-end uses the fitted model of the material and the selected machine using P ≤ 200 W area of the plot for the high-accuracy printing mode. Selecting low-accuracy implies achievable BVRs from the power range of 200 W < P < 1000 W.
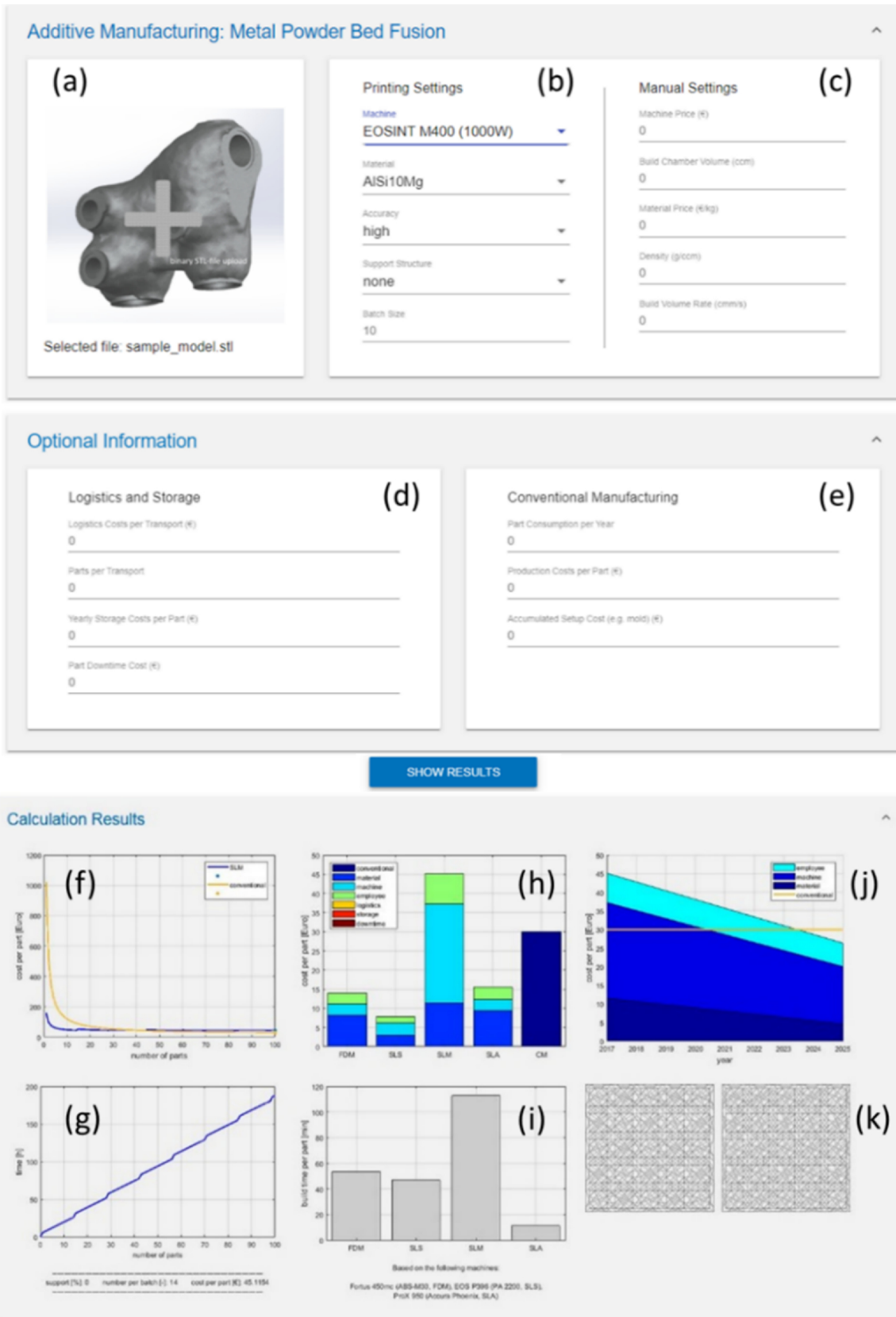
**Fig. 6.** The graphical user interface of the online tool "amdsp" (additively manufactured digital spare parts) for rapid dimensional, cost and lead time evaluations for metal-based PBF. (a) STL-file upload window, (b) print settings, (c) manual configurations, (d) logistic and storage considerations, (e) possibility to consider comparisons to conventionally produced parts, (f) cost per part analysis, (g) total time function, (h) cost structure comparison for four AM processes and conventional manufacturing, (i) process time comparison for four AM processes, (j) future cost projections, (k) frontal and side part preview.

**Fig. 7.** Generalized model adapted from [15]. Achievable BVRs as a function of the laser power for AlSi10Mg (Al), maraging steel DIN 1.2709 (St), and TiAl6V4 (Ti).

### 2.4. Analysis of data and model construction

The results of the DOE were analyzed using an ANOVA test with a confidence level of 95% ($\alpha = 0.05$). The test included first-order, second-order, and interaction terms in a full factorial to a second degre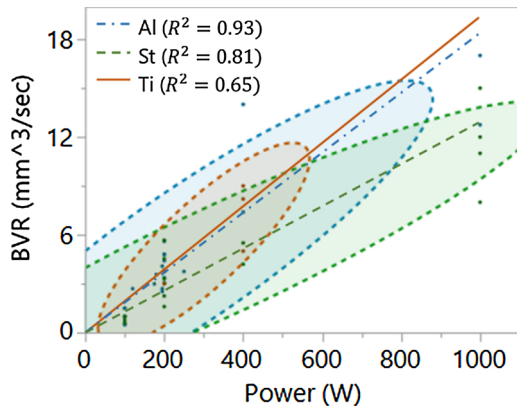e DOE. This involved a DOE with 108 experimental combinations simulated in the DSS and the online quotation system. The required manufacturing time per experimental combination was estimated by the DSS and therefore limited to the in-house production scenario. We fitted the experimental data to a surface response model (SRM). Eq. (2) defines the SRM model used to represent this relationship:

$$y = \beta_o + \sum_{i=1}^{k} \beta_i x_i + \sum_{i=1}^{k} \beta_{ii} x_i^2 + \sum_i \sum_j \beta_{ij} x_i x_j + \varepsilon \qquad (2)$$

Where, $\varepsilon$ is the unobserved random error, $\beta$ represent the coefficients of the regression model for each term (i.e. intercept $\beta_o$, first-order $\beta_i$, second-order $\beta_{ii}$, and the interaction term $\beta_{ij}$) calculated by the least square method, $x_i$ represent the independent variables LT, S, VF, PV, and M. The interaction terms between independent variables are represented by $x_i x_j$, and $y$ is the dependent variable (i.e. unit cost of production and manufacturing time).

The implemented model transforms the collected data into a model with reduced lack of fit, assuring that the prediction of the cost and manufacturing contains positive values, and follows a normal distribution with a constant variance. During the model construction, we defined S, VF, and PV as continuous variables and LT and M as categorical variables. We used a step-wise regression to eliminate non-significant variables and find the most parsimonious model. The stopping rule to determine model terms was set with a forward P-value threshold that uses the significance value of the term with a probability to enter of 0.25, which represents the maximum p-value that a term must have to be entered into the model during a forward step.

## 3. Results

### 3.1. The economic impact of lattice structures

Figs. 8 and 9 show the factor plot of the effect of the independent variables on the response, which is the effect of varying lattice type (LT), size (S), volume fraction (VF), production volume (PV), and material type (M) on the unit cost of production for both manufacturing scenarios (IN and OUT). For both factor plots, the standard error of

means, as well as the confidence interval, is presented.

The cost of in-house production is significantly lower than outsourcing. This is understandable as the cost of the outsourcing scenario includes the contribution margin on top of the manufacturing cost and additional overhead costs of the service bureau. The larger the difference between the minimum and maximum value of the mean effect at different levels, the higher is its significance and therefore influence over the response. By comparing the first-order effect of studied independent variables, in both cases IN and OUT, the variations of S and VF are the most significant terms for the unit cost of production. These two variables are responsible for the decrease in the volume of the part and therefore the required amount of material.

Similarly, in both manufacturing scenarios, the change in material drives the variation of the unit cost of production significantly. Results show consistently that processing Ti is more expensive than St and Al. The type of lattice design has little significance in cost variation in the IN scenario, while slightly affecting the OUT scenario. Similarly, the production volume has little significance on the costs in the IN scenario and significant influence on the variation of cost in the OUT scenario. This is due to the simulated high utilization rate of the in-house manufacturing scenario, which was 70%.

Table 2 shows the ANOVA test results of the included model terms for cost factors in both manufacturing scenarios by displaying the sum of squares, F-ratio, and P-value. The P-value is used to show the probability that measures the evidence against the null hypothesis. The lower the P-value, the stronger the evidence against the null hypothesis, which is the lack of statistical significance between specified populations. To this end, the ANOVA test shows that the effect of S, VF, and M is statistically significant (P-Value $\leq$ 0.001) for the variation of cost in both scenarios. Similarly, the comparison between both scenarios in terms of LT shows that LT significance is high for the OUT scenario, whereas in the IN scenario, the LT has no significance.

Another difference between first-order terms in the model for outsourcing and in-house production relates to the significance of PV. Nevertheless, the increase of PV has a positive effect on the decrease of cost in the in-house manufacturing scenario and especially in the outsourcing scenario as the unit cost of production is higher at low volumes (e.g. PV < 10 units) than at high volumes (e.g. PV > 90 units). The higher significance to the OUT scenario might be explained by price modifications as the manufacturing service bureau reduces the contribution margin when higher volumes are ordered.

Regarding interaction terms, the relationship between S and VF determines the amount of material used, which is the main cost driver in metal PBF. As a consequence, the interaction terms S*VF, S*M, and VF*M are the most significant interaction terms (P-Value $\leq$ 0.001) in both manufacturing scenarios. The fit of the model shows a $R^2$ adj. = 0.964 and $R^2$ adj. = 0.978 for in-house and outsourcing scenarios respectively. Figs. 10 and 11 show the impact of S, VF, and M in the unit cost of production for outsourcing (OUT) and in-house (IN) production scenarios, respectively.

The combination with the highest cost-saving potential in the IN scenario is LT = C, S = 1000 cm$^3$, VF = 0.15, PV = 100 units, and M = St, resulting in cost savings of 83.2%. All combinations with a VF = 0.15 and PV = 100 units show cost saving potential of more than 80%. The combination with the lowest savings potential is LT = C, S = 125 cm$^3$, VF = 0.3, PV = 1 unit, and M = Al that amounts to 40.4%.

In the OUT scenario, the highest cost-saving potential, 69.3%, is obtained when LT = C, S = 1000 cm$^3$, and VF = 0.15 for all materials and production volumes. The lowest potential for cost savings is obtained for LT = O, S = 125 cm$^3$, and VF = 0.3, also independent of materials and production volumes. In summary, full utilization of build

**Fig. 8.** First-order factor plot for lattice type (LT), part size (S), volume fraction (VF), production volume (PV), and material (M) impact in the in-house (IN) production scenario.



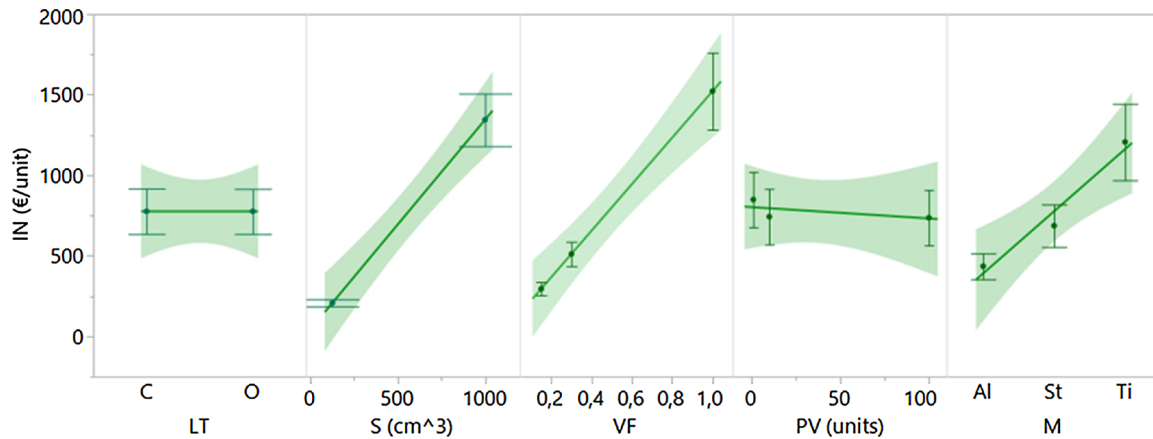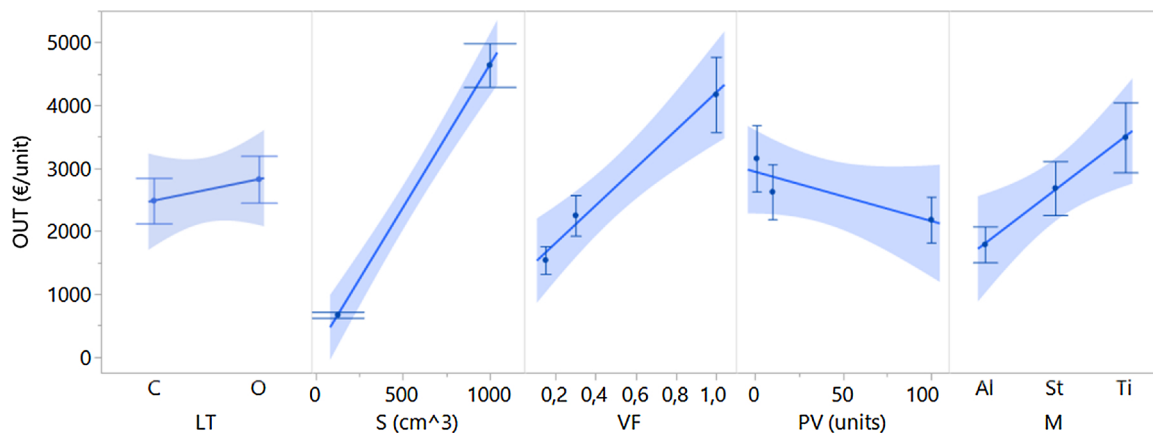**Fig. 9.** First-order factor plot for lattice type (LT), part size (S), volume fraction (VF), production volume (PV), and material (M) impact in the outsourcing (OUT) scenario.

platforms by manufacturing volume optimized parts, high production volumes, and implementation of lattices with low volume fractions lead to a substantial decrease of the unit cost of production in metal PBF. On average, lattice structures can decrease the unit cost of production by 70.6% and 52.9% for IN and OUT scenarios, respectively.

### 3.2. Manufacturing time and productivity impact of lattices structures

Fig. 12 shows the effect of varying lattice type (LT), size (S), volume fraction (VF), production volume (PV), and material type (M) on the manufacturing time. The factor plots show the standard error of means

**Table 2**
ANOVA table and SRM model report for the unit cost of production (€/unit). In-house (IN) versus outsourcing (OUT) production scenario.

| Source | DF | In-house (IN) | | | DF | Outsourcing (OUT) | | |
|---|---|---|---|---|---|---|---|---|
| | | Sum of Squares | F Ratio | P-value | | Sum of Squares | F Ratio | P-value |
| LT | – | – | – | – | 1 | 3129011 | 19,6365 | < 0,0001 |
| S | 1 | 34898510 | 936,4726 | < 0,0001 | 1 | 424913304 | 2666,603 | < 0,0001 |
| VF | 1 | 30895549 | 829,0565 | < 0,0001 | 1 | 41998622 | 263,5682 | < 0,0001 |
| PV | 1 | 241657 | 6,4847 | 0,0125 | 1 | 7792269 | 48,9015 | < 0,0001 |
| M | 2 | 11141727 | 149,4895 | < 0,0001 | 2 | 52148566 | 163,6328 | < 0,0001 |
| LT*S | – | – | – | – | 1 | 1934079 | 12,1376 | 0,0008 |
| LT*VF | – | – | – | – | 1 | 1445737 | 9,0729 | 0,0034 |
| S*VF | 1 | 18689950 | 501,5293 | < 0,0001 | 1 | 78952644 | 495,4783 | < 0,0001 |
| VF*VF | – | – | – | – | 1 | 1260757 | 7,9121 | 0,0061 |
| S*PV | – | – | – | – | 1 | 7386156 | 46,3528 | < 0,0001 |
| VF*PV | – | – | – | – | 1 | 2297927 | 14,421 | 0,0003 |
| PV*PV | 1 | 180203 | 4,8356 | 0,0303 | 1 | 3847345 | 24,1446 | < 0,0001 |
| S*M | 2 | 6716107 | 90,1106 | < 0,0001 | 2 | 29074963 | 91,232 | < 0,0001 |
| VF*M | 2 | 5912874 | 79,3335 | < 0,0001 | 2 | 9045554 | 28,3833 | < 0,0001 |
| PV*M | – | – | – | – | 2 | 906485 | 2,8444 | 0,0635 |
| Model | 11 | 108541961 | 264,7849 | – | 19 | 761785324 | 251,6153 | – |
| Error | 96 | 3577528 | – | – | 88 | 14022476 | – | – |
| C. Total | 107 | 112119489 | – | < 0,0001 | 107 | 775807800 | – | < 0,0001 |
| R$^2$ | | 0,968092 | | | | 0,981925 | | |
| R$^2$ adj. | | 0,964436 | | | | 0,978023 | | |
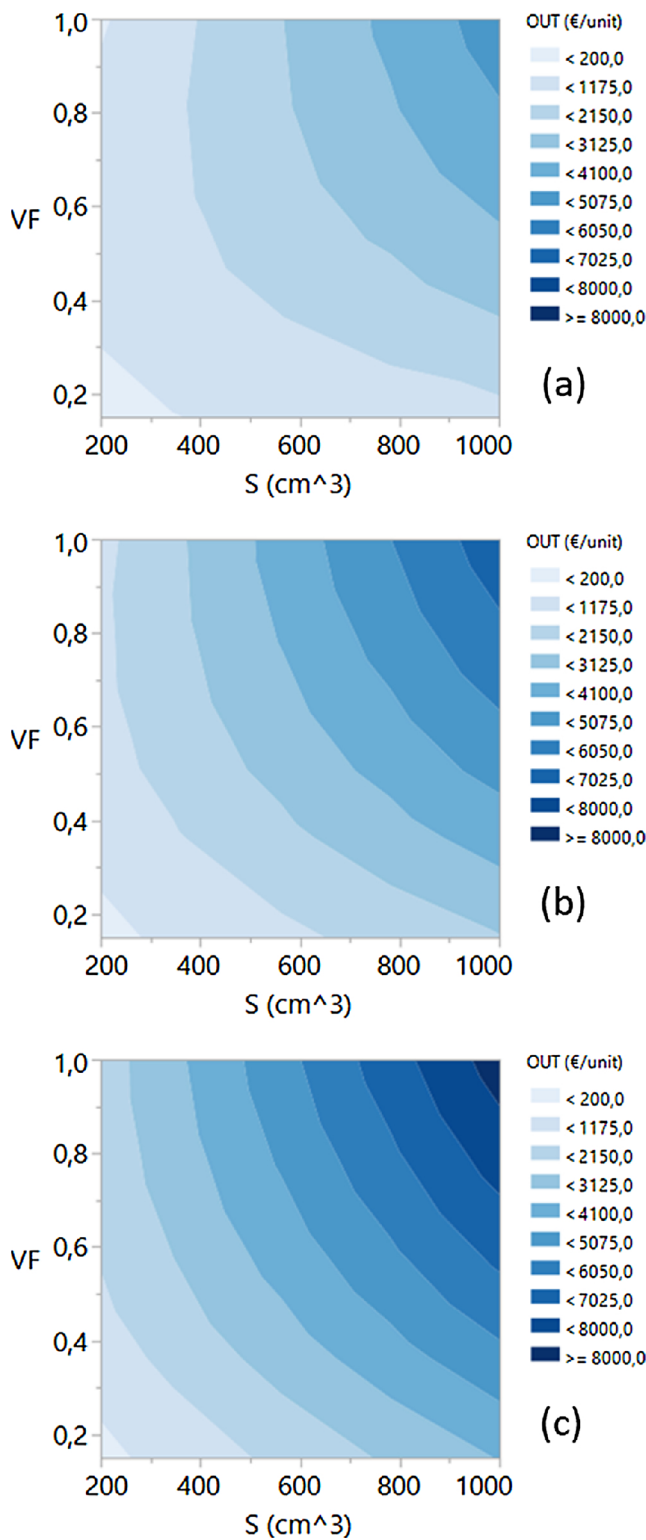
**Fig. 10.** Contour plots for the effect of S and VF on the unitary cost of production using outsourcing (OUT) manufacturing scenario in for (a) Al, (b) St, and (c) Ti.

**Fig. 11.** Contour plots for the effect of S and VF on the unitary cost of production using in-house (IN) manufacturing scenario for (a) Al, (b) St, and (c) Ti.

as well as the confidence interval. By comparing the first-order effect of studied independent variables, the variation of S and VF has the highest significance to the responding MT. S and VF are responsible for the decrease of the height and volume of the part, and therefore the

required amount of material. LT does not show a significant impact on MT, whereas the increase of PV has a positive effect on the overall MT due to the increased ability to utilize the build platform in each manufacturing batch fully. Each material has its own generalized BVR function and the results of the factor plot consistently show that the MT
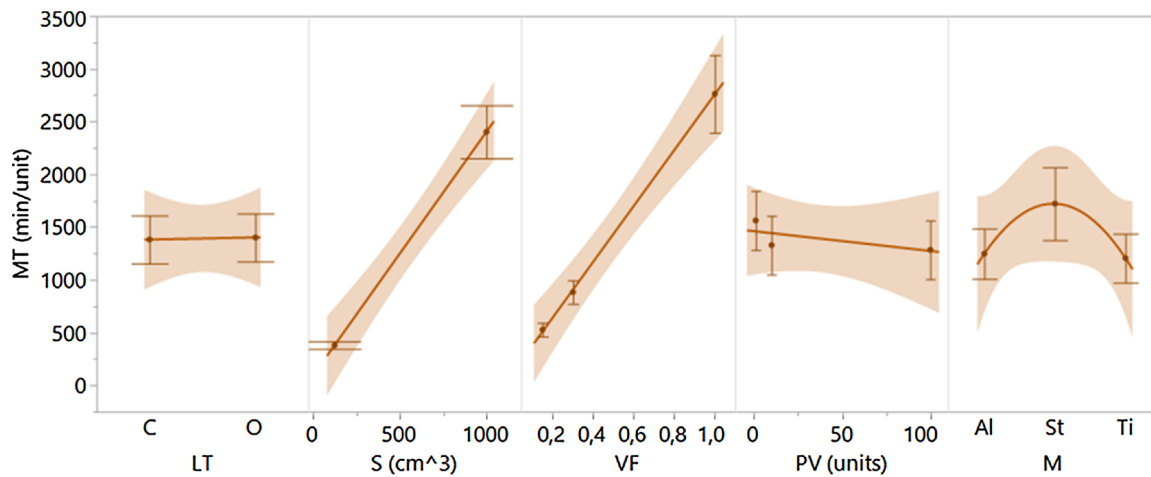
**Fig. 12.** First-order factor plot for lattice type (LT), part size (S), volume fraction (VF), production volume (PV), and material (M) impacts in manufacturing time (MT) per unit (min/unit).

**Table 3**
ANOVA table and SRM model report for manufacturing time (MT).

| Source | DF | Manufacturing time (MT) | | |
| --- | --- | --- | --- | --- |
| | | Sum of Squares | F Ratio | P-value |
| LT | – | – | – | – |
| S | 1 | 110413160 | 2812,232 | < 0,0001 |
| VF | 1 | 105868035 | 2696,467 | < 0,0001 |
| PV | 1 | 1226968 | 31,251 | < 0,0001 |
| M | 1 | 5875981 | 149,6617 | < 0,0001 |
| LT*S | – | – | – | – |
| LT*VF | – | – | – | – |
| S*VF | 1 | 62513189 | 1592,216 | < 0,0001 |
| VF*VF | – | – | – | – |
| S*PV | – | – | – | – |
| VF*PV | – | – | – | – |
| PV*PV | 1 | 851798 | 21,6954 | < 0,0001 |
| S*M | 1 | 3258031 | 82,9823 | < 0,0001 |
| VF*M | 1 | 4236591 | 107,9063 | < 0,0001 |
| PV*M | – | – | – | – |
| Model | 8 | 291637989 | 928,5054 | |
| Error | 99 | 3886913 | | |
| C. Total | 107 | 295524903 | | < 0,0001 |
| $R^2$ | | 0,986847 | | |
| $R^2$ adj. | | 0,985785 | | |

for Ti and Al is similar, whereas St requires more time for manufacturing.

As shown in Table 3, shows the ANOVA test results of the included model terms for MT as well as the sum of squares, F-ratio, and P-value. In connection to first-order terms, the interaction terms S*VF, S*M, and VF*M are the most significant ones (P-Value ≤ 0.001). The fit of the model describing the relationship between independent variables and the response of MT shows an $R^2$ adj. = 0.985.

The ANOVA test shows that the effect of S, VF, and M is statistically significant (P-Value ≤ 0.001) for the variation of MT, while LT term is not necessary for the model; and therefore, shows low statistical significance. On the other end, PV has a strong influence on MT. In relation to the effect of material in manufacturing time, the results replicate the BVR trend already introduced in Fig. 7. Fig. 13 outlines the impact of S, VF, and M on MT. The results displayed in the plot show that using lattice structures in metal PBF can significantly reduce the required MT.

Manufacturing time can be shortened by up to 88.1% when selecting the combination LT = C, S = 1000 cm³, VF = 0.15, and M = St.

### 3.3. Redesign by DfAM: a case study

To establish a baseline of potential cost and manufacturing time savings of DfAM in metal PBF, we study a case example of a mounting bracket from the brake system of a Corvette 1988-1996. This case is linked to the manufacture of an obsolete spare part that requires to be reverse-engineered and manufactured on demand due to the challenges of finding original spare part providers. The bracket redesign is used to evaluate and corroborate the findings of the DOE while assessing the potential benefits of DfAM integration with a realistic case example. The presented case study uses two DfAM approaches to redesign the bracket: (i) lightweight design by lattice structures, and (ii) topology optimization (TO).

Kantareddy, S. et al. [40] presents an analogous detailed design workflow to create a lightweight part with lattice structures using laser PBF process. During the re-design of the bracket by integrating lattice structures, the geometrical features with functionality are maintained intact. The assembly holes and the outer shell of the bracket were kept solid with a shell thickness of 3 mm to maintain its functionality. On the contrary, the inner part is emptied by integrating an octet-truss lattice design with volume fractions of 0.3 and 0.15. In relation to the manufacturability of these lattice structures, Fig. 3(b) demonstrates the ability to use metal PBF to build octet-truss lattice design with volume fractions of 0.15.

The TO version of the bracket design was obtained by defining the design space, loads, and boundary conditions (i.e. two bearing loads at the outer holes of the component of 3000 N each that mimics the contact force between a shaft and a bushing as well as two grounded sliding pins attached to the holes close to the center). During the TO, we used specific material models that correspond to Al, St, and Ti. The TO was performed in Altair Inspire. The assumption is that the material has an isotropic behavior. Assembly holes were kept solid with a minimum shell thickness of 3 mm to maintain the functionality of the bracket. Yoder, S. et al. [53] presents the detailed TO process flow involved in the FEA analysis.

The optimization objective is to minimize mass with a factor of safety of 1.5 to prevent the yielding of the obtained TO design due to stress. The TO study did not use additional constraints related to

(a)



(b)



(c)

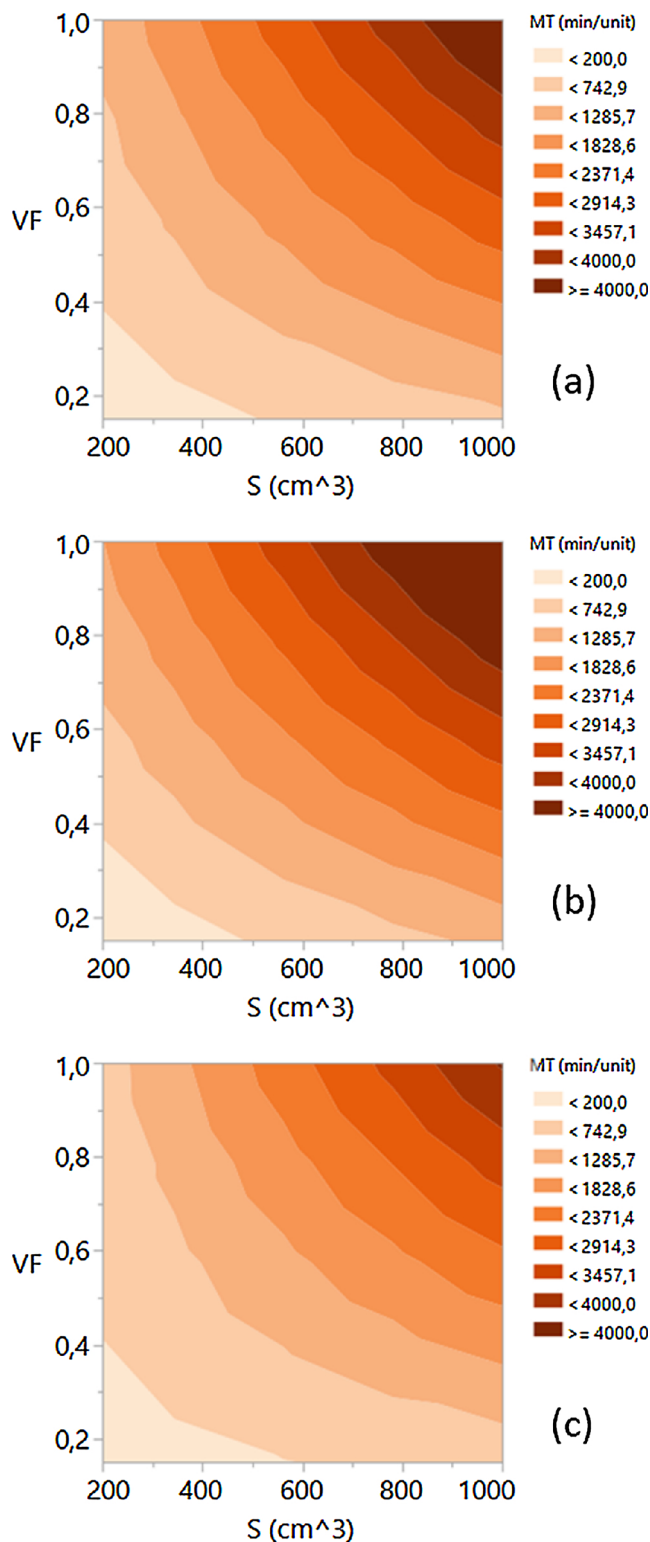**Fig. 13.** Contour plots for the effect of S and VF on manufacturing time (min/unit) for (a) Al, (b) St, and (c) Ti.

maximum displacement or stress. The resulting TO design will differ from material to material as well as the resulting part volume, mass, and mechanical behavior. Again, the principal objective of this DfAM case study is limited to study the productivity issues of the re-design by

lattice structures and TO; and therefore, we do not perform a mechanical performance study of the obtained designs. Table 4 shows the implemented material models as well as a schematic representation for the applied boundary conditions for the TO design.

Fig. 14 shows the results of the case study in terms of economics and productive of DfAM. The analysis is performed in the DSS, using the PBF system EOS M400 in the high-accuracy mode. Fig. 14(a) shows the cost reduction as a function of part mass, AM material, lattice VF, and TO results of the bracket made out of different materials. Fig. 14(b) shows the MT reduction as a function of part mass, AM material, lattice VF, and TO results of the bracket made of different materials. Fig. 14(c) illustrates the original design with a volume of 242.34 cm$^3$ and the perspective views of re-designs that include a lattice design and an exemplary TO part as well as the build direction of the part that is in z-axis. Finally, Fig. 14(d) shows descriptions of VFs for the bracket design with octet-truss lattices and the TO design.

The comparison of the DfAM for (i) lattice design and (ii) topology optimization results are presented in Table 5. The results show that unit cost of production using a lattice VF of 0.15 can decrease the cost of manufacturing by 57.4%, 59.4%, and 60% for Al, St, and Ti materials respectively. If more structurally sound design is required, a higher VF of 0.3 can be selected, in which case the cost of manufacturing decreases by 47.2%, 48.9%, and 49.3% for Al, St, and Ti materials respectively.

MT is also significantly reduced by using lattice structures. MT is reduced by 59.2%, 60.7%, and 58.7% for Al, St, and Ti materials, respectively, when using a VF of 0.15. Using a VF of 0.3 will allow reducing the MT by 49.1%, 49.7%, and 48.5% for Al, St, and Ti respectively. Similarly, TO design of the bracket considerably reduced the manufacturing cost by 68.1%, 69.7%, and 70.2% for Al, St, and Ti materials, respectively. MT decreases by 69.9%, 72.6%, and 68.9% for Al, St, and Ti materials, respectively.

Another positive impact of DfAM is the reduction of the overall weight of the original solid design. If we take a VF of 0.3 as a reference, the weight of the bracket design can be reduced by 52.5%, from 654 g to 310 g for Al, 1951 g to 926 g for St, and 1093 g to 518 g for Ti. Similarly, the TO version of the bracket reduces the overall weight of the part by 73.4%, 86.4%, and 85.5% for Al, St, and Ti respectively.
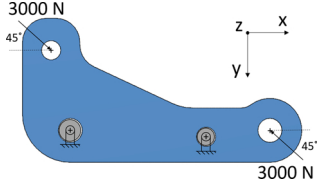
## 4. Discussion

In relation to the DOE results, both manufacturing scenarios: (i) in-house manufacturing assessed with the web-based DSS and (ii) outsourcing scenario evaluated by an online quotation system show very similar trends. For lattice design, part size (S) and lattice volume fraction (VF) are the most significant design variables that lead to the reduction of the unit cost of production and manufacturing time in metal PBF. The type of material used in AM has a significant effect on cost and manufacturing time. Whereas, lattice-type (LT) and production volume (PV) has a reduced significance in the variation of cost and manufacturing time. The relationship between part volume and lattice volume fraction determines the amount of material used, which is the main cost driver in metal PBF.

Integration of lattice structures leads to a substantial decrease in the unit cost of production as well as manufacturing time. Based on the results of the DOE, cost of production can decrease by 70.6% or 52.9% depending on the manufacturing scenario and design constraints. Similarly, manufacturing time can be reduced significantly by 71.7%, thus allowing even faster part delivery when DfAM is integrated adequately into engineering design phases. On average, the manufacturing cost can decrease by 53.7% and manufacturing time by 54.3% depending on the material and the volume fraction. The overall weight of the part is reduced by 52.5%.

**Table 4**

Material model and schematic of the boundary conditions for the re-design by TO of the bracket.

| Material | Young's modulus (Pa) | Poisson's ratio | Yield Stress (Pa) | Density (kg/m$^3$) |
|---|---|---|---|---|
| AlSi10Mg (Al) | 6.83E+10 | 0.3 | 1.80E+08 | 2.67E+03 |
| Maraging steel 1.2709 (St) | 1.30E+11 | 0.3 | 9.00E+08 | 8.00E+03 |
| Ti-6Al-4 V (Ti) | 1.17E+11 | 0.31 | 8.27E+08 | 4.43E+03 |

Schematic of the TO boundary conditions



Optimization objective: minimize mass with a factor of safety of 1.5

Assembly holes with a minimum solid shell thickness of 3 mm

Two bearing forces of 3000 N each in opposing directions with 45° degrees angles with the horizontal x-axis

Two constraints "grounded sliding pin" placed at center holes that allow rotation in the z-axis and constrains displacement in the y-axes and the x-axes
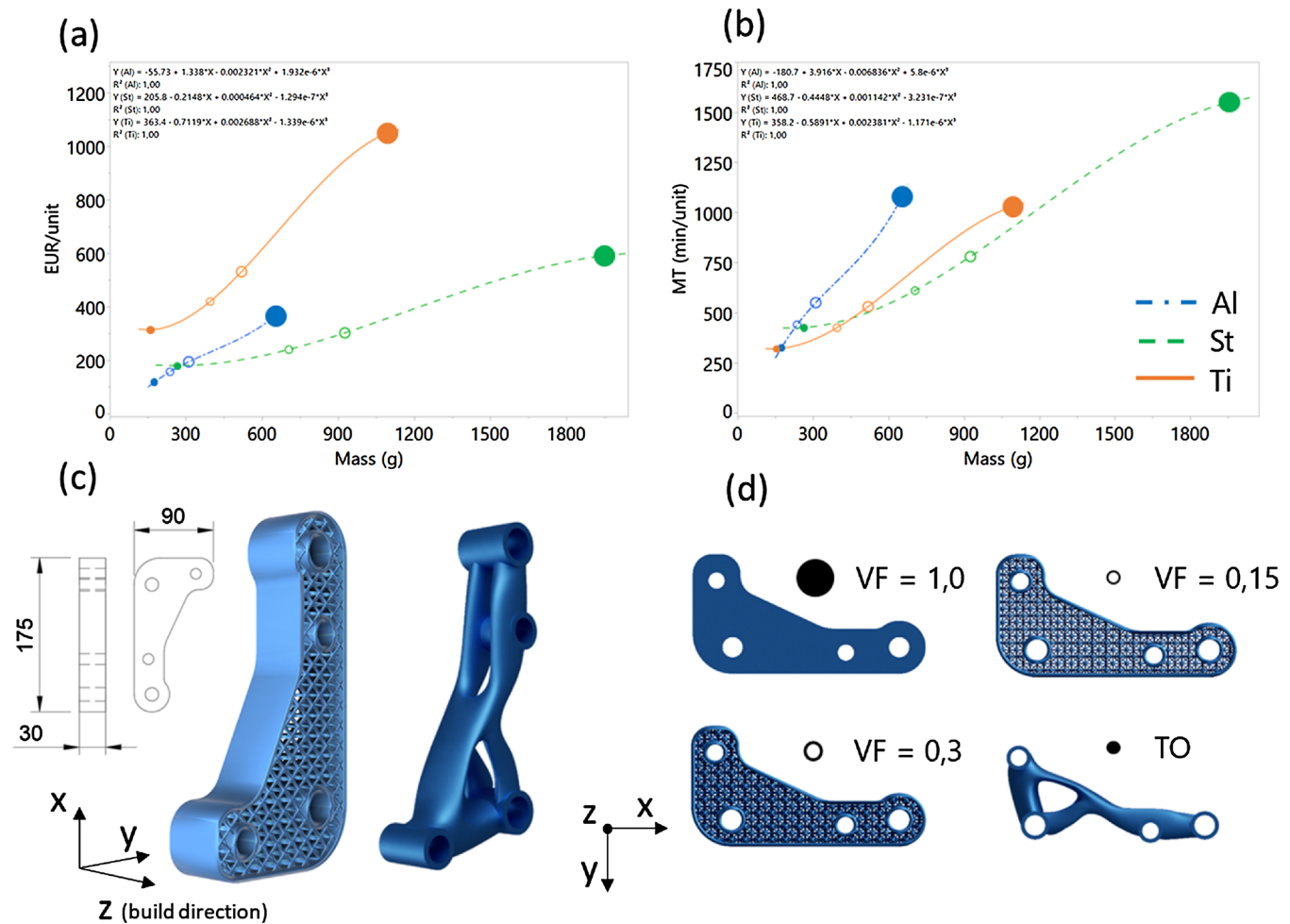


**Fig. 14.** Cost and MT savings of an example case of a bracket design. (a) Cost reduction as a function of part mass, AM material, and lattice VF, (b) MT reduction as a function of part mass, AM material, and lattice VF, (c) design space, perspective view of the lattice and TO design and dimensions of the bracket design, (d) description of VFs for the bracket design with octet-truss lattices and topologically optimized.

**Table 5**

Case study results for the cost, the manufacturing time and weight reduction.

| DfAM method | Cost reduction | | | MT reduction | | | Weight reduction | | |
|---|---|---|---|---|---|---|---|---|---|
| | Al | St | Ti | Al | St | Ti | Al | St | Ti |
| Lattice - VF = 0.15 | 57.4% | 59.4% | 60% | 59.2% | 60.7% | 58.7% | 63.8% | | |
| Lattice - VF = 0.3 | 47.2% | 48.9% | 49.3% | 49.1% | 49.7% | 48.5% | 52.5% | | |
| Topology optimization | 68.1% | 69.7% | 70.2% | 69.9% | 72.6% | 68.9% | 73.4% | 86.4% | 85.5% |

The case study on the bracket redesign shows that reduction of unitary cost of production and manufacturing time is strongly dependent on the ability to integrate DfAM opportunities in the engineering design process. Therefore, weight and material reduction through topology optimization, lattice structures or a combination of both are beneficial in reaching desired industrial efficiency for parts produced with AM. Overall, the re-design by DfAM of an existing part is a necessary step to make AM alternative advantageous. On average, the integration of lattices in the original bracket design reduces the cost of manufacturing by 53.7%. Similarly, the TO approach to re-design the bracket can reduce the unit cost of production by 59.8% on average.

Regarding the limitation of this research, we did not perform an in-depth study of the mechanical performance of the lattice designs or the TO alternative, which would be fundamental in evaluating the mechanical response and feasibility of the final designs [54]. Such analysis was out of the scope, whose purpose was to measure the value of DfAM quantitatively in terms of part cost and productivity.

This study has been limited to model potential manufacturing scenarios of direct part production, not considering the cost of additional post-processing steps, such as heat treatments for stress relief and machining operations for increased dimensional accuracy. The additional post-processing cost will be included in future versions of the online DSS. Furthermore, this research is limited to study the value of DfAM in part production in relation to design opportunities at the part level including micro-scale complexity (i.e. lattice, trusses, and cellular materials) and macro-scale complexity (i.e. material choice, freeform geometry, and topology optimization for functionality and performance). More research is required to measure the value of DfAM related to opportunities at the product level (i.e. part consolidation) [55].

There are several directions for future research. Overall, a systemic approach to DfAM is fundamental to industrialize AM. It is required to develop tailored methods to assess the technological and operational feasibility of the technology. In this context, the presented web-based DSS will be expanded and upgraded with more accurate back-end functions for BVRs to more precisely estimate the manufacturing cost and time of different materials. Instead of using a generalization based on high-accuracy versus low-accuracy as a function of the AM system laser power. We plan to model the typical process parameters (i.e. volumetric energy density based on power, scanning speed, layer thickness, and hatch distance) including the effect of contour scanning as an indicator for feature resolution to obtain more accurate BVR functions for different industrial materials and metal PBF machines.

Furthermore, the DSS is currently in expansion to enable continuous screening of inventories, including part information, such as size, material type, expected production volumes, storage, and logistics costs. These modifications will allow the screening of companies' part libraries to identify the most suitable candidates for metal PBF automatically. Another area of research is to analyze the impact of the machine utilization rate on the economic feasibility of the in-house manufacturing scenario. In the current version of the DSS, we assume a constant 70% utilization rate of the metal PBF system. Thus, future research should also conduct a sensitivity analysis by varying utilization rates to determine whether a company should invest in metal PBF or should keep the production of parts out-sourced. To this end, it is required to simulate real manufacturing scenarios related to demand forecasting of parts that would have an impact on the utilization rates of the metal PBF systems.

## 5. Conclusion

The decrease of the unit cost of production and manufacturing time are often crucial factors for the feasibility of metal PBF systems in industrial manufacturing scenarios. The parts need to be produced at an acceptable cost and delivered faster than potential conventionally produced counterparts. This study shows quantitatively how metal PBF technologies can become more competitive when integrating an alternative design approach using DfAM principles for lattice structures, topology optimization, or a combination of both. DfAM allows increasing the opportunities to find business cases for direct part production using metal PBF

The results of this study show that full utilization of build platforms by manufacturing volume optimized parts, high production volumes, and reduction of volume fraction leads to substantial benefits for metal PBF industrialization. DfAM is a necessary step to industrialize AM to be able to design manufacturable lattice designs or topologically optimized structures with reduced part volume that lead to optimized part production cost and manufacturing time in metal PBF. The obtained designs need to fulfil the mechanical and geometrical requirements of the intended application.

Our research demonstrates the value of DfAM in terms of cost, manufacturing lead time, and productivity. This should encourage firms to actively redesign parts of existing products for AM, design parts for new products for AM, and have a sizeable portfolio of parts which can be produced by AM. Firms can also simultaneously decide whether to invest in AM equipment in-house or outsource or use a combination of both. It is also important to acknowledge that the optimal supply model of AM production (i.e. in-house, outsourcing, or mixed model) has to consider a holistic AM part portfolio perspective, DfAM capabilities, specifics on best-suited AM technologies, as well as the business models of the company. Taking decisions sequentially on isolated case studies may result in sub-optimal outcomes. Therefore, there is a need for comprehensive methodologies and decision support tools to facilitate such advanced decision making.

## Declaration of Competing Interest

Authors declare that this work does not represent any kind of conflict of interest.

## Acknowledgements

## Appendix A

**Table A1**

Collected data set for the outsourcing scenario (OUT) using an online quotation system, and in-house scenario (IN) utilizing a decision support system.

| # | LT | S | VF | PV | M | (OUT) €/unit | (IN) €/unit | (MT) min / part |
|---|---|---|---|---|---|---|---|---|
| 1 | C | 125 | 0 | 1 | Al | 815,71 | 295,36 | 780 |
| 2 | C | 125 | 0 | 1 | St | 1223,57 | 409,94 | 1000 |
| 3 | C | 125 | 0 | 1 | Ti | 1590,64 | 642,33 | 750 |
| 4 | C | 125 | 0 | 10 | Al | 678,48 | 183,83 | 530 |
| 5 | C | 125 | 0 | 10 | St | 1017,72 | 298,41 | 790 |
| 6 | C | 125 | 0 | 10 | Ti | 1323,04 | 530,8 | 520 |
| 7 | C | 125 | 0 | 100 | Al | 564,33 | 180,72 | 520 |
| 8 | C | 125 | 0 | 100 | St | 846,5 | 295,3 | 780 |
| 9 | C | 125 | 0 | 100 | Ti | 1100,45 | 527,69 | 510 |
| 10 | C | 125 | 0,15 | 1 | Al | 296,87 | 150,44 | 330 |
| 11 | C | 125 | 0,15 | 1 | St | 445,31 | 168,75 | 365 |
| 12 | C | 125 | 0,15 | 1 | Ti | 578,91 | 210,33 | 330 |
| 13 | C | 125 | 0,15 | 10 | Al | 246,93 | 38,91 | 103 |
| 14 | C | 125 | 0,15 | 10 | St | 370,39 | 57,22 | 138 |
| 15 | C | 125 | 0,15 | 10 | Ti | 481,51 | 98,8 | 100 |
| 16 | C | 125 | 0,15 | 100 | Al | 205,39 | 35,8 | 96 |
| 17 | C | 125 | 0,15 | 100 | St | 308,08 | 54,11 | 135 |
| 18 | C | 125 | 0,15 | 100 | Ti | 400,51 | 95,69 | 95 |
| 19 | C | 125 | 0,3 | 1 | Al | 417,78 | 176 | 410 |
| 20 | C | 125 | 0,3 | 1 | St | 626,66 | 211,29 | 485 |
| 21 | C | 125 | 0,3 | 1 | Ti | 814,66 | 286,53 | 405 |
| 22 | C | 125 | 0,3 | 10 | Al | 347,49 | 64,47 | 180 |
| 23 | C | 125 | 0,3 | 10 | St | 521,24 | 99,76 | 250 |
| 24 | C | 125 | 0,3 | 10 | Ti | 677,61 | 175 | 165 |
| 25 | C | 125 | 0,3 | 100 | Al | 289,03 | 61,36 | 166 |
| 26 | C | 125 | 0,3 | 100 | St | 433,55 | 96,65 | 245 |
| 27 | C | 125 | 0,3 | 100 | Ti | 563,61 | 171,89 | 170 |
| 28 | C | 1000 | 0 | 1 | Al | 5875,03 | 1514,25 | 4450 |
| 29 | C | 1000 | 0 | 1 | St | 8812,54 | 2429,59 | 6300 |
| 30 | C | 1000 | 0 | 1 | Ti | 11456,3 | 4280,81 | 4300 |
| 31 | C | 1000 | 0 | 10 | Al | 4886,63 | 1413,66 | 4200 |
| 32 | C | 1000 | 0 | 10 | St | 7329,95 | 2329,01 | 6050 |
| 33 | C | 1000 | 0 | 10 | Ti | 9528,94 | 4180,22 | 4050 |
| 34 | C | 1000 | 0 | 100 | Al | 4064,53 | 1403,96 | 4150 |
| 35 | C | 1000 | 0 | 100 | St | 6096,79 | 2319,3 | 6030 |
| 36 | C | 1000 | 0 | 100 | Ti | 7925,83 | 4170,52 | 4030 |
| 37 | C | 1000 | 0,15 | 1 | Al | 1802,76 | 354,91 | 950 |
| 38 | C | 1000 | 0,15 | 1 | St | 2704,14 | 500,04 | 1230 |
| 39 | C | 1000 | 0,15 | 1 | Ti | 3515,38 | 824,79 | 930 |
| 40 | C | 1000 | 0,15 | 10 | Al | 1499,47 | 254,32 | 710 |
| 41 | C | 1000 | 0,15 | 10 | St | 2249,21 | 399,46 | 1000 |
| 42 | C | 1000 | 0,15 | 10 | Ti | 2923,97 | 724,21 | 698 |
| 43 | C | 1000 | 0,15 | 100 | Al | 1247,2 | 244,62 | 700 |
| 44 | C | 1000 | 0,15 | 100 | St | 1870,81 | 389,75 | 995 |
| 45 | C | 1000 | 0,15 | 100 | Ti | 2432,05 | 714,5 | 680 |
| 46 | C | 1000 | 0,3 | 1 | Al | 2746,98 | 559,39 | 1580 |
| 47 | C | 1000 | 0,3 | 1 | St | 4120,47 | 840,37 | 2100 |
| 48 | C | 1000 | 0,3 | 1 | Ti | 5356,61 | 1434,36 | 1500 |
| 49 | C | 1000 | 0,3 | 10 | Al | 2284,84 | 458,81 | 1320 |
| 50 | C | 1000 | 0,3 | 10 | St | 3427,26 | 739,79 | 1800 |
| 51 | C | 1000 | 0,3 | 10 | Ti | 4455,44 | 1333,78 | 1290 |
| 52 | C | 1000 | 0,3 | 100 | Al | 1900,45 | 449,1 | 1300 |
| 53 | C | 1000 | 0,3 | 100 | St | 2850,67 | 730,09 | 720 |
| 54 | C | 1000 | 0,3 | 100 | Ti | 3705,87 | 1324,07 | 1250 |
| 55 | O | 125 | 0 | 1 | Al | 815,71 | 295,36 | 780 |
| 56 | O | 125 | 0 | 1 | St | 1223,57 | 409,94 | 1000 |
| 57 | O | 125 | 0 | 1 | Ti | 1590,64 | 642,33 | 750 |
| 58 | O | 125 | 0 | 10 | Al | 678,48 | 183,83 | 530 |
| 59 | O | 125 | 0 | 10 | St | 1017,72 | 298,41 | 790 |
| 60 | O | 125 | 0 | 10 | Ti | 1323,04 | 530,8 | 520 |
| 61 | O | 125 | 0 | 100 | Al | 564,33 | 180,72 | 520 |
| 62 | O | 125 | 0 | 100 | St | 846,5 | 295,3 | 780 |
| 63 | O | 125 | 0 | 100 | Ti | 1100,45 | 527,69 | 510 |
| 64 | O | 125 | 0,15 | 1 | Al | 376,91 | 150,47 | 330 |
| 65 | O | 125 | 0,15 | 1 | St | 565,36 | 168,8 | 365 |
| 66 | O | 125 | 0,15 | 1 | Ti | 734,97 | 210,43 | 210 |
| 67 | O | 125 | 0,15 | 10 | Al | 313,5 | 38,95 | 105 |
| 68 | O | 125 | 0,15 | 10 | St | 470,25 | 57,27 | 139 |
| 69 | O | 125 | 0,15 | 10 | Ti | 611,32 | 98,9 | 100 |
| 70 | O | 125 | 0,15 | 100 | Al | 260,76 | 35,84 | 96 |
| 71 | O | 125 | 0,15 | 100 | St | 391,14 | 54,17 | 135 |

*(continued on next page)*

**Table A1** (*continued*)

| # | LT | S | VF | PV | M | (OUT) €/unit | (IN) €/unit | (MT) min / part |
|---|----|---|----|----|---|-------------|------------|-----------------|
| 72 | O | 125 | 0,15 | 100 | Ti | 508,48 | 95,79 | 95 |
| 73 | O | 125 | 0,3 | 1 | Al | 512,73 | 175,9 | 405 |
| 74 | O | 125 | 0,3 | 1 | St | 769,1 | 211,12 | 485 |
| 75 | O | 125 | 0,3 | 1 | Ti | 999,83 | 286,22 | 400 |
| 76 | O | 125 | 0,3 | 10 | Al | 426,47 | 64,37 | 180 |
| 77 | O | 125 | 0,3 | 10 | St | 639,71 | 99,59 | 250 |
| 78 | O | 125 | 0,3 | 10 | Ti | 831,62 | 174,69 | 175 |
| 79 | O | 125 | 0,3 | 100 | Al | 354,72 | 61,26 | 175 |
| 80 | O | 125 | 0,3 | 100 | St | 532,08 | 96,48 | 248 |
| 81 | O | 125 | 0,3 | 100 | Ti | 691,71 | 171,59 | 170 |
| 82 | O | 1000 | 0 | 1 | Al | 5875,03 | 1514,25 | 4450 |
| 83 | O | 1000 | 0 | 1 | St | 8812,54 | 2429,59 | 6300 |
| 84 | O | 1000 | 0 | 1 | Ti | 11456,3 | 4280,81 | 4300 |
| 85 | O | 1000 | 0 | 10 | Al | 4886,63 | 1413,66 | 4200 |
| 86 | O | 1000 | 0 | 10 | St | 7329,95 | 2329,01 | 6050 |
| 87 | O | 1000 | 0 | 10 | Ti | 9528,94 | 4180,22 | 4050 |
| 88 | O | 1000 | 0 | 100 | Al | 4064,53 | 1403,96 | 4150 |
| 89 | O | 1000 | 0 | 100 | St | 6096,79 | 2319,3 | 6030 |
| 90 | O | 1000 | 0 | 100 | Ti | 7925,83 | 4170,52 | 4030 |
| 91 | O | 1000 | 0,15 | 1 | Al | 2469,89 | 355,17 | 950 |
| 92 | O | 1000 | 0,15 | 1 | St | 3704,83 | 500,48 | 1220 |
| 93 | O | 1000 | 0,15 | 1 | Ti | 4816,28 | 825,58 | 920 |
| 94 | O | 1000 | 0,15 | 10 | Al | 2054,36 | 254,59 | 720 |
| 95 | O | 1000 | 0,15 | 10 | St | 3081,55 | 399,9 | 1000 |
| 96 | O | 1000 | 0,15 | 10 | Ti | 4006,01 | 725 | 695 |
| 97 | O | 1000 | 0,15 | 100 | Al | 1708,74 | 244,89 | 700 |
| 98 | O | 1000 | 0,15 | 100 | St | 2563,12 | 390,2 | 995 |
| 99 | O | 1000 | 0,15 | 100 | Ti | 3332,05 | 715,3 | 680 |
| 100 | O | 1000 | 0,3 | 1 | Al | 3541,82 | 558,58 | 1560 |
| 101 | O | 1000 | 0,3 | 1 | St | 5312,72 | 839,02 | 2150 |
| 102 | O | 1000 | 0,3 | 1 | Ti | 6906,54 | 1431,94 | 1500 |
| 103 | O | 1000 | 0,3 | 10 | Al | 2945,95 | 457,99 | 1330 |
| 104 | O | 1000 | 0,3 | 10 | St | 4418,93 | 738,44 | 1850 |
| 105 | O | 1000 | 0,3 | 10 | Ti | 5744,61 | 1331,35 | 1280 |
| 106 | O | 1000 | 0,3 | 100 | Al | 2450,34 | 448,29 | 1300 |
| 107 | O | 1000 | 0,3 | 100 | St | 3675,51 | 728,73 | 1800 |
| 108 | O | 1000 | 0,3 | 100 | Ti | 4778,16 | 1321,65 | 1260 |

## References

[1] R.Y. Zhong, X. Xu, E. Klotz, S.T. Newman, Intelligent manufacturing in the context of industry 4.0: a review, Engineering 3 (2017) 616–630, https://doi.org/10.1016/J.ENG.2017.05.015.

[2] V. Petrovic, J. Vicente Haro Gonzalez, O. Jordá Ferrando, J. Delgado Gordillo, J. Ramón Blasco Puchades, L. Portolés Griñan, Additive layered manufacturing: sectors of industrial application shown through case studies, Int. J. Prod. Res. 49 (2011) 1061–1079, https://doi.org/10.1080/00207540903479786.

[3] M.K. Niaki, S.A. Torabi, F. Nonino, Why manufacturers adopt additive manufacturing technologies: the role of sustainability, J. Clean. Prod. 222 (2019) 381–392, https://doi.org/10.1016/j.jclepro.2019.03.019.

[4] M.K. Thompson, G. Moroni, T. Vaneker, G. Fadel, R.I. Campbell, I. Gibson, A. Bernard, J. Schulz, P. Graf, B. Ahuja, F. Martina, Design for Additive Manufacturing: trends, opportunities, considerations, and constraints, CIRP Ann. Manuf. Technol. 65 (2016) 737–760, https://doi.org/10.1016/j.cirp.2016.05.004.

[5] I. Flores Ituarte, N. Kretzschmar, S. Chekurov, J. Partanen, J. Tuomi, Additive manufacturing validation methods, technology transfer based on case studies, in: E. Pei, M. Monzón Verona, A. Bernard (Eds.), Addit. Manuf. – Dev. Train. Educ. Springer International Publishing, 2018, pp. 99–112 https://www.springer.com/it/book/9783319760834.

[6] S. Chekurov, T. Lantela, Selective laser melted digital hydraulic valve system, 3D print, Addit. Manuf. 4 (2017) 215–221, https://doi.org/10.1089/3dp.2017.0014.

[7] S. Chekurov, J. Kajaste, K. Saari, H. Kauranne, M. Pietola, J. Partanen, Additively manufactured high-performance counterflow heat exchanger, Prog. Addit. Manuf. 4 (2018) 55–61, https://doi.org/10.1007/s40964-018-0059-x.

[8] I. Flores Ituarte, S.H. Khajavi, J. Partanen, Challenges to implementing additive manufacturing in globalised production environments, Int. J. Collab. Enterp. 5 (2016) 232–247.

[9] J. Bonnín Roca, P. Vaishnav, R.E. Laureijs, J. Mendonça, E.R.H. Fuchs, Technology cost drivers for a potential transition to decentralized manufacturing, Addit. Manuf. 28 (2019) 136–151, https://doi.org/10.1016/j.addma.2019.04.010.

[10] D. Strong, M. Kay, B. Conner, T. Wakefield, G. Manogharan, Hybrid manufacturing – integrating traditional manufacturers with additive manufacturing (AM) supply chain, Addit. Manuf. 21 (2018) 159–173, https://doi.org/10.1016/j.addma.2018.03.010.

[11] I. Flores Ituarte, S. Chekurov, J. Tuomi, J. Etienne Mascolo, A. Zanella, P. Springer, J. Partanen, Digital manufacturing applicability of a laser sintered component for automotive industry: a case study, Rapid Prototyp. J. (2018), https://doi.org/10.1108/RPJ-11-2017-0238.

[12] S.H. Khajavi, J. Partanen, J. Holmström, Additive manufacturing in the spare parts supply chain, Comput. Ind. 65 (2014) 50–63, https://doi.org/10.1016/j.compind.2013.07.008.

[13] D. Rosen, What are Principles for Design for Additive Manufacturing? 1st Int. Conf. Prog. Addit. Manuf. (May) (2014) 26–28, https://doi.org/10.3850/978-981-09-0446-3 (Pro-AM 2014), n.d.

[14] R.M. Ballardini, I. Flores Ituarte, E. Pei, Printing spare parts through additive manufacturing: legal and digital business challenges, J. Manuf. Technol. Manag. 29 (2018) 958–982, https://doi.org/10.1108/MRR-09-2015-0216.

[15] N. Kretzschmar, I. Flores Ituarte, J. Partanen, A decision support system for the validation of metal powder bed-based additive manufacturing applications, Int. J. Adv. Manuf. Technol. (2018) 12.

[16] M. Ruffo, C. Tuck, R. Hague, Make or buy analysis for rapid manufacturing, Rapid Prototyp. J. 13 (2007) 23–29, https://doi.org/10.1108/13552540710719181.

[17] S. Hällgren, L. Pejryd, J. Ekengren, (Re)Design for additive manufacturing, Procedia Cirp 50 (2016) 246–251, https://doi.org/10.1016/j.procir.2016.04.150.

[18] N. Kretzschmar, S. Chekurov, The applicability of the 40 TRIZ principles in design for additive manufacturing, 29th DAAAM Proc. (2018) 0888–0893, https://doi.org/10.2507/29th.daaam.proceedings.128.

[19] M. Baumers, L. Beltrametti, A. Gasparre, R. Hague, Informing additive manufacturing technology adoption : total cost and the impact of capacity utilisation, Int. J. Prod. Res. 7543 (2017) 0, https://doi.org/10.1080/00207543.2017.1334978.

[20] M. Ruffo, C. Tuck, R. Hague, Cost estimation for rapid manufacturing-laser sintering production for low to medium volumes, Proc. Inst. Mech. Eng. Part B J. Eng. Manuf. 220 (2006) 1417–1427.

[21] E. Atzeni, L. Iuliano, P. Minetola, A. Salmi, Redesign and cost estimation of rapid manufactured plastic parts, Rapid Prototyp. J. 16 (2010) 308–317, https://doi.org/10.1108/13552541011065704.

[22] Y. Zhang, A. Bernard, J.M. Valenzuela, K.P. Karunakaran, Fast adaptive modeling method for build time estimation in Additive Manufacturing, CIRP J. Manuf. Sci. Technol. 10 (2015) 49–60, https://doi.org/10.1016/j.cirpj.2015.05.003.

[23] EOS GmbH - Electro Optical Systems, EOS 400-4: Ultra-fast quad-laser system for industrial 3D printing, (n.d.).,2018 https://www.eos.info/systems_solutions/eos-m-

400-4 (accessed November 28, 2018).

[24] T.H.J. Vaneker, The role of Design for Additive Manufacturing in the successful economical introduction of AM, Procedia Cirp 60 (2017) 181–186, https://doi.org/10.1016/j.procir.2017.02.012.

[25] M. Suard, Characterization and Optimization of Lattice Structures Made by Electron beam Melting, (2015), pp. 1–233, https://doi.org/10.1177/0964663912467814.

[26] A. Hadi, F. Vignat, F. Villeneuve, Design configurations and creation of lattice structures for metallic additive manufacturing, 14ème colloq. Natl. AIP PRIMECA, La Plagne, France, 2015.

[27] J. Mun, B.G. Yun, J. Ju, B.M. Chang, Indirect additive manufacturing based casting of a periodic 3D cellular metal - Flow simulation of molten aluminum alloy, J. Manuf. Process. 17 (2015) 28–40, https://doi.org/10.1016/j.jmapro.2014.11.001.

[28] L. Dong, V. Deshpande, H. Wadley, Mechanical response of Ti-Al-4V octet-truss lattice structures, Int. J. Solids Struct. 60 (2015) 107–124, https://doi.org/10.1016/j.ijsolstr.2015.02.020.

[29] D.T. Queheillalt, H.N.G. Wadley, Cellular metal lattices with hollow trusses, Acta Mater. 53 (2005) 303–313, https://doi.org/10.1016/j.actamat.2004.09.024.

[30] H.N.G. Wadley, N.A. Fleck, A.G. Evans, Fabrication and structural performance of periodic cellular metal sandwich structures, Compos. Sci. Technol. 63 (2003) 2331–2343, https://doi.org/10.1016/S0266-3538(03)00266-5.

[31] B. Vayre, F. Vignat, F. Villeneuve, Designing for additive manufacturing, Procedia Cirp 3 (2012) 632–637, https://doi.org/10.1016/j.procir.2012.07.108.

[32] B. Vayre, F. Vignat, F. Villeneuve, Metallic additive manufacturing: state-of-the-art review and prospects, Mech. Ind. 76 (2012) 611–613, https://doi.org/10.1051/meca/2012003.

[33] A.H. Azman, F. Vignat, F. Villeneuve, CAD tools and file format performance evaluation in designing lattice structures for additive manufacturing, J. Teknol. 80 (2018) 87–95, https://doi.org/10.11113/jt.v80.12058.

[34] A.H. Azman, F. Vignat, F. Villeneuve, Evaluating current CAD tools performances in the context of design for additive manufacturing, Jt. Conf. Mech. (2014) 1–7, https://doi.org/10.1080/10934529.2011.579857.

[35] C. Yan, L. Hao, A. Hussein, D. Raymont, Evaluations of cellular lattice structures manufactured using selective laser melting, Int. J. Mach. Tools Manuf. 62 (2012) 32–38, https://doi.org/10.1016/j.ijmachtools.2012.06.002.

[36] A. Emelogu, M. Marufuzzaman, S.M. Thompson, N. Shamsaei, L. Bian, Additive manufacturing of biomedical implants: a feasibility assessment via supply-chain cost analysis, Addit. Manuf. 11 (2016) 97–113, https://doi.org/10.1016/j.addma.2016.04.006.

[37] D. Hub, How to design parts for metal 3D printing 3D hubs, 3D Print. Handb. (2018) (Accessed April 30, 2019), https://www.3dhubs.com/knowledge-base/how-design-parts-metal-3d-printing.

[38] S. Kim, D.W. Rosen, P. Witherell, H. Ko, A design for additive manufacturing ontology to support manufacturability analysis, ASME 2018 Int. Des. Eng. Tech. Conf. Comput. Inf. Eng. Conf. Quebec City, Quebec, Canada, 2018 p. 10. doi:978-0-7918-5175-3.

[39] I. Gibson, D. Rosen, B. Stucker, Additive Manufacturing Technologies: 3D Printing, Rapid Prototyping, and Direct Digital Manufacturing, 2nd ed., Springer Science +Business Media, New York, 2015.

[40] S.N.R. Kantareddy, B.M. Roh, T.W. Simpson, S. Joshi, C. Dickman, E.A. Lehtihet, Saving weight with metallic lattice structures: design challenges with a Real-world example, Proc. Solid Free. Fabr. Symp. (2016) 2139–2154.

[41] M. Baumers, P. Dickens, C. Tuck, R. Hague, The cost of additive manufacturing: machine productivity, economies of scale and technology-push, Technol. Forecast. Soc. Change 102 (2016) 193–201, https://doi.org/10.1016/j.techfore.2015.02.015.

[42] M. Schmidt, M. Merklein, D. Bourell, D. Dimitrov, T. Hausotte, K. Wegener, L. Overmeyer, F. Vollertsen, G.N. Levy, Laser based additive manufacturing in industry and academia, CIRP Ann. Manuf. Technol. 66 (2017) 561–583, https://doi.org/10.1016/j.cirp.2017.05.011.

[43] W. Gao, Y. Zhang, D. Ramanujan, K. Ramani, Y. Chen, C.B. Williams, C.C.L. Wang, Y.C. Shin, S. Zhang, P.D. Zavattieri, The status, challenges, and future of additive manufacturing in engineering, Comput. Des. (2015), https://doi.org/10.1016/j.cad.2015.04.001.

[44] Materialise, Materialise OnSite | 3D Prototypes - Onsite - Home, (n.d.).,2018 https://onsite.materialise.com/en (Accessed May 7, 2019).

[45] B. Michael, J. Sanjay, S. Timothy, D. Corey, Cost modeling and depreciation for reused powder feedstocks in powder bed fusion additive manufacturing, Proc. 27th Annu. Int. Solid Free. Fabr. Symp. 44 (2013) 52–54 http://content.wkhealth.com/linkback/openurl?sid=WKPTLP:landingpage&an=00006247-201303000-00012.

[46] V. Petrovic, J. Vicente Haro Gonzalez, O. Jordá Ferrando, J. Delgado Gordillo, J. Ramon Blasco Puchades, L. Portoles Grinan, Additive layered manufacturing: sectors of industrial application shown through case studies, Int. J. Prod. Res. 49 (2011) 1061–1079, https://doi.org/10.1080/00207540903479786.

[47] W.E. Frazier, Metal additive manufacturing: a review, J. Mater. Eng. Perform. 23 (2014) 1917–1928, https://doi.org/10.1007/s11665-014-0958-z.

[48] W.J. Sames, F.A. List, S. Pannala, R.R. Dehoff, S.S. Babu, The metallurgy and processing science of metal additive manufacturing, Int. Mater. Rev. 6608 (2016) 1–46, https://doi.org/10.1080/09506608.2015.1116649.

[49] T. DebRoy, H.L. Wei, J.S. Zuback, T. Mukherjee, J.W. Elmer, J.O. Milewski, A.M. Beese, A. Wilson-Heid, A. De, W. Zhang, Additive manufacturing of metallic components – process, structure and properties, Prog. Mater. Sci. 92 (2018) 112–224, https://doi.org/10.1016/j.pmatsci.2017.10.001.

[50] M. Tang, P.C. Pistorius, J.L. Beuth, Prediction of lack-of-fusion porosity for powder bed fusion, Addit. Manuf. 14 (2017) 39–48, https://doi.org/10.1016/j.addma.2016.12.001.

[51] M. Megahed, H.-W. Mindt, N. N'Dri, H. Duan, O. Desmaison, Metal additive-manufacturing process and residual stress modeling, Integr. Mater. Manuf. Innov. (2016), https://doi.org/10.1186/s40192-016-0047-2.

[52] A.M. Rubenchik, W.E. King, S.S. Wu, Scaling laws for the additive manufacturing, J. Mater. Process. Technol. 257 (2018) 234–243, https://doi.org/10.1016/j.jmatprotec.2018.02.034.

[53] S. Yoder, S. Morgan, C. Kinzy, E. Barnes, M. Kirka, V. Paquit, P. Nandwana, A. Plotkowski, R.R. Dehoff, S.S. Babu, Characterization of topology optimized Ti-6Al-4V components using electron beam powder bed fusion, Addit. Manuf. 19 (2018) 184–196, https://doi.org/10.1016/j.addma.2017.12.001.

[54] M.E. Lynch, M. Mordasky, L. Cheng, A. To, Design, testing, and mechanical behavior of additively manufactured casing with optimized lattice structure, Addit. Manuf. 22 (2018) 462–471, https://doi.org/10.1016/j.addma.2018.05.021.

[55] M.K. Thompson, G. Moroni, T. Vaneker, G. Fadel, R.I. Campbell, I. Gibson, A. Bernard, J. Schulz, P. Graf, B. Ahuja, F. Martina, Design for Additive Manufacturing: trends, opportunities, considerations, and constraints, CIRP Ann. Manuf. Technol. 65 (2016) 737–760, https://doi.org/10.1016/j.cirp.2016.05.004.